Article

The Glass Mosaic of *S. Agnese fuori le mura*: New Tesserae in the Puzzle of Early Medieval Rome

Alberta Silvestri [1,*], Sarah Maltoni [2], Manuela Gianandrea [3], Rita Deiana [4] and Chiara Croci [2]

1   Department of Geosciences, University of Padua, Via G. Gradenigo 6, 35131 Padua, Italy
2   Section of Art History, Faculty of Arts, University of Lausanne, Anthropole 4143, 1005 Lausanne, Switzerland
3   Department of History, Antropology, Religions, Art History, Media and Performing Arts,
    Sapienza University of Rome, Piazzale Aldo Moro 5, 00168 Rome, Italy
4   Department of Cultural Heritage, University of Padua, Piazza Capitaniato 7, 35139 Padua, Italy
*   Correspondence: alberta.silvestri@unipd.it

Abstract: The present study, which is part of a wider inter-disciplinary research project on Medieval Rome funded by the Swiss National Science Foundation, focuses on the archaeometric characterisation of glass tesserae from the apse mosaic of the church of *S. Agnese fuori le mura*, dated to the 7th century AD and never analysed until now. The main aims of the study are the identification of chemical compositions of glassy matrices and colouring/opacifying techniques by means of the combination of micro-textural, chemical, and mineralogical data. In *S. Agnese* tesserae, the results show the presence of glassy matrices and opacifiers/pigments, typical of both Roman and Late Antique/Early Medieval periods. The technological features identified (in particular, glassy matrices and opacifiers/pigments) allow us to discriminate not only new-production tesserae, i.e., those probably produced in the 7th century for the realisation of the *S. Agnese* mosaic, but also those obtained from recycling or re-using previous glass. This testifies to a quite complex "puzzle", unusual in other glass mosaics from the same city and coeval with *S. Agnese*, supporting further the potentiality of archaeometric studies on glass to uncover the technical and socio-cultural knowledge that underpins its manufacturing, use, re-use, and recycling in the Early Medieval Rome.

Keywords: glass mosaic; Early Medieval period; Rome; archaeometry; glassy matrix; opacifier/pigment; colouring element; new production tesserae; re-use; recycling

1. Introduction

The glass mosaics of Late Antique and Medieval Rome (Italy) were the object of numerous conservation and restoration campaigns in recent decades, which often allowed the sampling and analysis of tesserae. The studies carried out from 1991 to 2004 on mosaics from Rome, dated between the 4th and 13th centuries AD, were all collected and published in 2017 in a book edited by Andaloro and D'Angelo [1]. This book constitutes an important reference dataset for understanding the evolution of the mosaic technique and glass tesserae chemical compositions in an exceptional context, such as the city of Rome.

The apse mosaic of the church of *S. Agnese fuori le mura* in Rome, commissioned by Pope Honorius I (625–638), is not included in this volume because its tesserae were never studied from the archaeometric point of view until now. Therefore, the present study, which is part of a wider inter-disciplinary research project on Medieval Rome funded by the Swiss National Science Foundation and focuses on the archaeometric characterisation of the glass tesserae from *S. Agnese fuori le mura*, dated to the 7th century AD, aims to fill this knowledge gap. By combining micro-textural, chemical, and mineralogical data, glassy matrices and colouring/opacifying techniques were, in particular, investigated. The present results allowed not only to implement the inter-disciplinary research conducted so far on Late Antique and Medieval glass, thanks to the acquisition of new data on raw materials, production technologies, and commercial routes, to be compared to those

previously obtained on other mosaics of Rome and outside Rome, but also to emphasise the potentiality of archaeometric studies on glass to uncover the technical and socio-cultural knowledge that underpins its manufacturing, use, re-use, and recycling in the Early Medieval Rome.

2. The Glass Mosaic of *S. Agnese fuori le mura* from the Art-Historical Viewpoint

The mosaic of *S. Agnese fuori le mura* is the cornerstone of the extensive project undertaken by Pope Honorius I within the complex of buildings founded in Constantinian times along the via *Nomentana* [2]. The basilica arises, in fact, above the tomb of the main Roman female martyr, Agnes, whose image is the central focus of the apse mosaic (Figure 1).

Figure 1. Rome, *S. Agnese fuori le mura*, apse mosaic (625–638), © Domenico Ventura.

The synthetic and hieratic composition of the mosaic dominated by the titular saint is what distinguishes *S. Agnese* from other Roman apses of the Middle Ages. For the prevailing gold background as well as for the use of stone tesserae to realise the martyr's face, the mosaic has been regarded as a breakpoint in the Roman artistic production of the early Middle Ages and considered as a result of the Byzantine taste arrived in Rome under the imperial administration ruling the city since the middle of 6th century. In our previous research, we have summarised the historiographical question and demonstrated the relation between the synthetic iconography of the mosaic and the choice, rather new for the time, of placing the martyr saint in the centre of the apse, at the focal point of the basilica. We have also shown that the gold background and the use of stone tesserae for Agnes' face need to be understood as precise aesthetic choices within the context of a wisely orchestrated space [3,4]. Those advancements have been possible in the wake of other recent developments focusing on the entanglement between the mosaic and the architectural setting, as well as on his relation to the audience taking part in the liturgy performed in the basilica [5–7].

Given the weight of precise rhetorical choices on the formal—'stylistic'—outcome of the mosaic, it seemed to us essential to investigate production technologies. The in-depth study of the glass tesserae of the mosaic presented in this article is thus an essential step to acquire more specific information on the context of *S. Agnese*'s mosaic making and to place it within the technological practices of Rome and the Early Medieval West.

3. Materials and Methods

3.1. Materials

The apse mosaic of *S. Agnese fuori le mura* has a complex history because, in the past, it was heavily restored, and this complicates the identification of the original parts, the object of the present study. Therefore, preliminary investigations were carried out by means of visual analysis, archival research, and non-invasive methods, such as multispectral imaging. By combining the results of the preliminary investigations, the original areas of the *S. Agnese* mosaic were identified [8], from which some tesserae were chosen and sampled for the laboratory analyses, discussed in Section 3.2.

The tesserae were taken from different points of the mosaic, taking care to characterise the original areas, as detected by preliminary investigations, and all the colours identified: gold, blue, white, green, yellow, purple, and red/orange. To ensure a characterisation of the mosaic as complete as possible, at least two tesserae were selected for each colour, except for the orange one, which was identified in very limited areas. Finally, some erratic tesserae were also selected; a total of 46 tesserae were sampled (34 in situ and 12 erratic) (Table 1; see also Figures 6 and 7 in Deiana et al. [8]). It should be stressed here that the number of tesserae from *S. Agnese fuori le mura*, the object of archaeometric analyses, is the highest one, never selected before from a single mosaic in Rome.

The sampling procedure of the tesserae from the apse mosaic of *S. Agnese fuori le mura* is detailed in Deiana et al. [8]. Here it is only remarked that, for the lab analyses, a layer about 1 mm in thickness was cut with a diamond-coated micro-saw from the back of each opaque coloured tessera and from the side in the case of the gold ones, to allow the sampling of both supporting tessera, gold foil, and cartellina, when present.

3.2. Methods

The glass tesserae from *S. Agnese fuori le mura* mosaic were investigated by means of a laboratory analytical protocol, already applied to other in situ glass mosaics, such as the paleo-Christian mosaic of *S. Maria Mater Domini* in Vicenza and the Byzantine Dedication wall mosaic located in the Church of St. Mary of the Admiral in Palermo [9,10]. The analytical protocol is multi-methodological and includes Optical Microscopy (OM) for preliminary morphological observations, Scanning Electron Microscopy, coupled with Energy-Dispersive Spectrometry (SEM-EDS) for high-resolution morphologic inspection of glass and qualitative chemical analyses, Electron Probe Micro-Analysis (EPMA) to determine quantitative chemical composition of glassy matrix, and X-ray Powder Diffraction (XRPD) to define the crystalline phases of opacifiers/pigments used in the tesserae.

OM observations were conducted under stereoscopic vision (OM-St) with a Zeiss Stemi 2000C microscope (Carl Zeiss, Oberkochen, Germany) and under reflected light (OM-RL) with a Nikon EclipseMe600 (Nikon Corporation, Tokyo, Japan).

The instruments employed for SEM-EDS analyses were two: the first, located in the Department of Geociences of the University of Padua, is a CamScan MX 2500 microscope (Electron Optic Services Inc., Ottawa, Canada) equipped with a LaB_6 cathode and an EDAX energy-dispersive X-ray spectrometer. The second instrument, located in the CNR-ICMATE building of Padua, is an FEI Quanta 200 FEG-ESEM instrument (Thermo Fisher Scientific, Waltham, MA, USA) equipped with a Genesys energy-dispersive X-ray spectrometer. In both the instruments, SEM images were taken by collecting the backscattered electron signal (BSE), operating under high-vacuum conditions (<4 Pa), with an accelerating voltage of 20 kV and a working distance (WD) of about 25 mm in the case of CamScan MX 2500 microscope, and an accelerating voltage of 25 kV and a WD of approximately 10 mm, in the case of the FEI Quanta 200 FEG-ESEM.

Table 1. List of *S. Agnese fuori le mura* tesserae, selected for archaeometric analyses, subdivided by colour macro-group. Colour, NCS code, diaphaneity, sampling area and some notes are also reported. n.a.: not applicable.

Colour Macro-Group	Label	Colour	NCS Code	Diaphaneity	Sampling Area	Notes
Gold	SA Au1	pale yellow-green	n.a.	transparent	Background on the left of *Onorio*	Only supporting tessera: no gold foil and cartellina.
	SA Au2	colourless	n.a.	transparent	Background between *Onorio* and *Agnese*	Only gold foil and cartellina: no supporting tessera.
	SA Au3	colourless	n.a.	transparent	Background between *Onorio* and *Agnese*	Only supporting tessera: no gold foil and cartellina.
	SA Au4	colourless	n.a.	transparent	Background between *Onorio* and *Agnese*	Only gold foil and cartellina: no supporting tessera.
	SA Au5	colourless	n.a.	transparent	Background between *Onorio* and *Agnese* near church	Only supporting tessera: no gold foil and cartellina.
	SA Au6	colourless	n.a.	transparent	Background between *Onorio* and *Agnese* near church	Only supporting tessera: no gold foil and cartellina.
	SA Au7	pale green	n.a.	transparent	Background between *Agnese* and *Simmaco*	Only supporting tessera: no gold foil and cartellina.
	SA Au8	pale green	n.a.	transparent	Background between *Agnese* and *Simmaco*	Complete gold tessera.
	SA Au9	colourless	n.a.	transparent	Erratic	Complete gold tessera.
Blue	SA B1	blue	S4050-R80B	opaque	meadow (dark green) between *Simmaco* and *Agnese*	
	SA B2	blue	S3050-R80B	opaque	meadow (dark green) near the left foot of *Simmaco*	
	SA B3	blue	S4550-R80B	semi-opaque	Erratic	
	SA B4	blue	S4550-R80B	semi-opaque	Erratic	
	SA B5	blue	S3560-R80B	semi-opaque	Erratic	
	SA B6	blue	S3560-R80B	opaque	Erratic	
	SA B7	blue	S5040-R80B	opaque	Erratic	
	SA B8	blue	S5040-R80B	semi-opaque	Erratic	
	SA B9	blue	S5040-R80B	opaque	Erratic	
	SA Tu1	turquoise	S3060-B10G	opaque	meadow (dark green) on the left of *Onorio*, over the second letter "a" of the word "aurea".	
	SA Tu2	turquoise	S3060-B10G	opaque	meadow (dark green) on the left of *Onorio*, over the first letter "s" of the word "concisis".	
White	SA Bi1	white	S1000N	opaque	*Simmaco—pallio*	
	SA Bi2	white	S1000N	opaque	*Onorio—pallio*	
	SA Bi3	white	S1002-Y	opaque	Erratic	
	SA Gr1	grey	S2502-Y	opaque	*Onorio*—church, low part between two doors.	
	SA Gr2	grey	S2502-Y	opaque	*Simmaco—pallio*	

Table 1. *Cont.*

Colour Macro-Group	Label	Colour	NCS Code	Diaphaneity	Sampling Area	Notes
Purple	SA P1	purple	S 6010-R30B	opaque	*Agnese* dress—Right sleeve	
	SA P2	dark purple	S 8505-R80B	semi-opaque	*Agnese* dress—Left sleeve	located very close to SA-P4
	SA P3	pale purple-pink	S5010-Y70R	semi-opaque	*Onorio* dress—under the church and right-hand	
	SA P4	greyish purple	S5010 R10B	opaque	*Agnese* dress—Left sleeve	located very close to SA-P2
	SA P5	pale purple-pink	S5020-R	semi-opaque	*Simmaco* dress—Left sleeve	
	SA P6	dark purple	S 8505-R80B	translucent	*Simmaco pallio*—under the book	
	SA R4	purple	S8010-Y90R	translucent	Erratic	
Green	SA VCh1	pale green	S3010- G1Y0 GL	opaque	meadow (light)—near the feet of *Onorio*	
	SA VCh2	pale green	S 2010-G40Y GL	opaque	meadow (light)—between *Onorio* and *Agnese*	located very close to SA-VCh3
	SA VCh3	pale green	S 2010-G70Y GL	opaque	meadow (light)—between *Onorio* and *Agnese*	
	SA VCh4	pale green	S 2020 G50Y	opaque	meadow (light) on the left of the low part of *Onorio*'s dress	located very close to SA-G2
	SA VCh5	pale green	S3030-G10Y	opaque	Erratic	
	SA VS1	dark green	S6010-G10Y	opaque	meadow (dark)—under the right feet of *Onorio*	
	SA VS2	dark green	S5020-G10Y	opaque	meadow (dark)—under the right feet of *Onorio*	located very close to SA-VS3
	SA VS3	dark green	S5030-G30Y	opaque	meadow (dark)—under the right feet of *Onorio*	located very close to SA-VS2
Yellow	SA G1	yellow	S2060-Y	opaque	Gold background over meadow (light) on the left of *Onorio*	
	SA G2	yellow	S2050-Y10R	opaque	Meadow (light) on the left of the low part of *Onorio*'s dress	located very close to SA-VCh4
Red/orange	SA A1	orange	S2050-Y50R	opaque	Flames on the left of *Agnese*	
	SA R1	dark red	S6030-R	opaque	*Onorio*—dress (in the centre)	
	SA R2	red	S2570-Y80R	opaque	*Onorio*—roof of the church	
	SA R3	red	S3060-Y90R	opaque	Erratic	

Quantitative chemical analyses, aimed at acquiring data on major and minor elements characterising the glassy matrix of *S. Agnese fuori le mura* assemblage avoiding the inclusions (i.e., opacifiers/pigments and/or relict crystalline phases), were carried out by using EPMA. The instrument employed was a JEOL 8200 Super Probe (JEOL (Italia) S.p.A., Basiglio, Italy), equipped with five WDS spectrometers and located at the Department of Earth Sciences of the University of Milan "La Statale". Analytical conditions used for *S. Agnese* tesserae are detailed in Table S1a, provided as Supplementary Materials. The accuracy of EPMA measures was checked against the international reference standards, Corning glasses A and B [11], and was lower than 1% for SiO_2, Na_2O, CaO, and K_2O lower than 5% for Al_2O_3, MgO, Fe_2O_3 and Sb_2O_3, lower than 10% for TiO_2, MnO, P_2O_5, and CuO, and within 20% for other minor elements; details of the measures on standard glasses are reported in Table S1b (Supplementary Materials). The quantitative chemical compositions of glassy matrices of the *S. Agnese fuori le mura* tesserae were identified through about six/ten point-microanalyses for each sample, and averages and standard deviations were calculated.

XRPD analyses were carried out on opaque tesserae (35 of 46 tesserae) using a PANalytical X'Pert PRO diffractometer (Bragg-Brentano geometry) (Malvern PANalytical, Almelo, The Netherlands) equipped with CoKα X-ray tube (λ = 1.7902 Å), operating at 40 kV and 40 mA. The scans are collected in the angular range 3°–80° 2 θ with a 0.03° virtual step size and a 100 s/step counting time. XRPD analytical data were processed using the X'Pert HighScore, version 3.0.5 (PANalytical copyright); 2θ and d values were calculated with the second-derivative algorithm of Savitzky and Golay [12].

While OM-St and XRPD were performed on the whole layers from each sampled tessera for conservative purposes, part of the layers was then embedded into resin blocks for OM-RL, SEM, EPMA, and, in the case of SEM and EPMA, the blocks were also coated with a thin carbon layer.

4. Results and Discussion

4.1. Glassy Matrix

The full chemical composition of the glassy matrix of tesserae from *S. Agnese fuori le mura*, as obtained using the EPMA analyses and subdivided by colour macro-group, is reported in Table 2. In the case of the complete gold tesserae, SA Au8 and SA Au9, the cartellina and the supporting tessera were analysed separately (see SA Au8 cartellina, SA Au8 supporting tessera, and SA Au9 cartellina, SA Au9 supporting tessera in Table 2), but, having a comparable composition, the mean composition of each whole tessera is calculated (see SA Au8* and SA Au9* in Table 2), and these will be discussed in the following paragraphs.

In accordance with the classification method proposed by Fiori et al. [13] for Byzantine glass mosaic and based on the $PbO/(SiO_2 + Na_2O + CaO)$ ratio, the majority of *S. Agnese* tesserae are composed of a glassy matrix, soda-lime in composition ($PbO/(SiO_2 + Na_2O + CaO) < 0.01$). Some tesserae, in particular those green, yellow and grey in colour, are soda-lime-lead in composition, having $PbO/(SiO_2 + Na_2O + CaO)$ ratio between 0.01 and 0.1, and two tesserae SA A1 and SA R2, orange and red in colour, respectively, are made of lead glass ($PbO/(SiO_2 + Na_2O + CaO) > 0.1$ in both cases) (Table 2). The relatively high lead content (PbO > 1 wt%) of lead and soda-lime-lead glassy matrices appears linked to colouring/opacifying techniques and/or other technological factors, as detailed in sub-Section 4.2.

Considering that mosaic tesserae, especially opaque and intentionally coloured ones, were produced by incorporating colouring elements and opacifying agents or pigments into a base glass, altering the full chemical composition of the glassy matrix, the base glass interpretation was performed on a reduced composition. This involved removing trace and intentionally adding elements associated with colour and opacity, i.e., CoO, NiO, CuO, Sb_2O_3 and PbO (Table S2 in Supplementary Materials), following the method outlined in Silvestri et al. [14]. To prevent confusion when discussing chemical data, elements in the reduced composition are denoted with an asterisk (*).

Table 2. Full mean chemical compositions of *S. Agnese* tesserae, listed by colour macro-group (EPMA data, expressed as oxide weight percentage). Note that Cr_2O_3 and NiO contents were measured but not reported here because, in all tesserae, they are below the EPMA detection limits, equal to 0.03 wt% in both cases. $PbO/(SiO_2 + Na_2O + CaO)$ ratio and classification of the glassy matrix in accordance with Fiori et al. [13] also included.

Colour Macro-Group	Sample	Colour	SiO₂ (wt%)	Na₂O (wt%)	CaO (wt%)	Al₂O₃ (wt%)	K₂O (wt%)	MgO (wt%)	Fe₂O₃ (wt%)	TiO₂ (wt%)	MnO (wt%)	P₂O₅ (wt%)	SO₃ (wt%)	Cl (wt%)	CoO (wt%)	CuO (wt%)	SnO₂ (wt%)	Sb₂O₃ (wt%)	PbO (wt%)	Total	PbO/(SiO₂ + Na₂O + CaO)	Glassy Matrix
Gold	SA Au1	pale yellow-green	70.49	18.87	5.63	2.12	0.49	0.50	0.37	0.06	0.15	0.09	0.20	1.15	<0.03	<0.04	<0.04	0.44	<0.06	100.55	0.00	Soda-lime
	SA Au2	colourless	71.40	18.35	5.93	1.85	0.35	0.51	0.38	0.07	0.54	0.06	0.26	1.17	<0.03	<0.04	<0.04	0.11	<0.06	100.99	0.00	Soda-lime
	SA Au3	colourless	70.38	18.64	5.94	2.09	0.49	0.49	0.33	0.07	0.14	0.09	0.20	1.13	<0.03	<0.04	<0.04	0.51	<0.06	100.49	0.00	Soda-lime
	SA Au4	colourless	70.66	15.78	7.10	2.49	0.51	0.58	0.40	0.08	1.40	0.13	0.12	0.88	<0.03	<0.04	<0.04	<0.03	<0.06	100.12	0.00	Soda-lime
	SA Au5	colourless	64.68	21.35	6.41	2.34	0.37	0.85	0.67	0.15	1.19	0.06	0.28	1.27	<0.03	<0.04	<0.04	<0.03	<0.06	99.62	0.00	Soda-lime
	SA Au6	colourless	64.25	21.68	6.45	2.30	0.39	0.89	0.67	0.14	1.18	0.06	0.29	1.32	<0.03	<0.04	<0.04	<0.03	<0.06	99.61	0.00	Soda-lime
	SA Au7	pale green	67.87	18.53	6.95	2.48	0.50	0.75	0.59	0.13	1.08	0.08	0.19	1.10	<0.03	<0.04	<0.04	<0.03	<0.06	100.25	0.00	Soda-lime
	SA Au8 *	pale green	68.15	18.69	6.48	2.27	0.43	0.67	0.54	0.11	0.96	0.09	0.17	1.19	<0.03	<0.04	<0.04	<0.03	<0.06	99.73	0.00	Soda-lime
	SA Au9 *	colourless	64.99	19.04	6.36	2.62	0.32	1.54	1.32	0.30	2.22	0.05	0.20	1.07	<0.03	<0.04	<0.04	<0.03	<0.06	100.02	0.00	Soda-lime
Blue	SA B1	blue	67.11	18.31	6.45	2.16	0.47	0.57	1.20	0.09	0.38	0.10	0.21	1.17	0.10	0.20	<0.04	1.07	0.71	100.31	0.01	Soda-lime
	SA B2	blue	67.66	16.35	6.87	2.49	0.74	0.59	0.95	0.10	0.57	0.13	0.22	0.77	0.11	0.19	<0.04	1.63	0.49	99.86	0.01	Soda-lime
	SA B3	blue	66.50	18.44	6.55	2.51	0.43	1.01	1.64	0.26	0.75	0.09	0.19	1.01	0.07	0.22	<0.04	0.31	0.27	100.23	0.00	Soda-lime
	SA B4	blue	67.06	18.56	6.88	2.57	0.59	0.79	1.21	0.18	0.67	0.09	0.25	1.08	0.05	0.18	<0.04	0.32	0.19	100.67	0.00	Soda-lime
	SA B5	blue	69.29	18.23	6.48	2.22	0.46	0.65	1.15	0.10	0.12	0.14	0.18	1.11	0.03	0.28	<0.04	0.42	<0.06	100.87	0.00	Soda-lime
	SA B6	blue	67.06	16.76	6.95	2.44	0.73	0.57	1.02	0.09	0.56	0.15	0.22	0.77	0.13	0.22	<0.04	1.58	0.53	99.79	0.01	Soda-lime
	SA B7	blue	67.62	14.69	6.57	2.31	0.53	0.56	1.34	0.03	0.89	0.16	0.26	0.58	0.27	0.29	<0.04	2.66	1.37	100.15	0.02	Soda-lime-lead
	SA B8	blue	67.91	17.69	6.82	2.66	0.64	0.88	1.13	0.21	0.69	0.13	0.19	1.00	0.04	0.10	<0.04	0.53	0.15	100.78	0.00	Soda-lime
	SA B9	blue	68.91	16.76	6.12	2.23	0.70	0.61	1.11	0.12	0.45	0.18	0.15	1.02	0.10	0.21	<0.04	1.32	0.33	100.33	0.00	Soda-lime
	SA Tu1	turquoise	68.49	17.97	3.37	2.15	0.42	0.64	1.11	0.17	0.02	0.06	0.15	1.12	<0.03	3.46	0.15	0.98	0.08	100.34	0.00	Soda-lime
	SA Tu2	turquoise	68.39	17.96	3.82	2.21	0.44	0.68	0.96	0.17	0.01	0.08	0.13	1.09	<0.03	3.73	0.14	0.95	0.08	100.82	0.00	Soda-lime
White	SA Bi1	white	66.71	17.58	5.49	2.13	0.57	3.22	0.50	0.05	0.03	0.04	0.31	0.68	<0.03	<0.04	<0.04	2.80	<0.06	100.11	0.00	Soda-lime
	SA Bi2	white	67.89	16.35	5.74	2.03	0.49	3.06	0.53	0.06	0.03	0.07	0.26	0.64	<0.03	<0.04	<0.04	2.88	<0.06	100.04	0.00	Soda-lime
	SA Bi3	white	66.68	17.57	5.48	2.18	0.57	3.11	0.47	0.05	0.03	0.07	0.28	0.68	<0.03	<0.04	<0.04	2.83	<0.06	99.98	0.00	Soda-lime
	SA Gr1	grey	63.34	19.48	7.26	2.09	0.43	0.85	0.90	0.23	1.13	0.16	0.18	1.31	<0.03	<0.04	1.00	<0.03	1.67	100.02	0.02	Soda-lime-lead
	SA Gr2	grey	62.81	19.94	6.27	2.13	0.45	0.80	0.85	0.19	1.16	0.08	0.26	1.16	<0.03	<0.04	1.39	<0.03	2.64	100.13	0.03	Soda-lime-lead
Purple	SA P1	purple	68.39	16.90	6.19	2.21	0.56	0.68	0.49	0.07	2.30	0.08	0.32	0.66	<0.03	<0.04	<0.04	1.14	0.09	100.07	0.00	Soda-lime
	SA P2	dark purple	65.90	18.54	6.43	2.66	0.53	1.05	1.26	0.36	2.14	0.08	0.20	1.04	<0.03	<0.04	<0.04	0.06	0.16	100.41	0.00	Soda-lime
	SA P3	pale purple-pink	68.87	18.59	6.02	2.32	0.53	0.65	0.58	0.12	0.57	0.08	0.25	1.10	<0.03	<0.04	<0.04	0.46	0.07	100.18	0.00	Soda-lime
	SA P4	greyish purple	67.66	17.48	6.01	2.22	0.62	0.88	0.59	0.09	1.63	0.09	0.28	0.74	<0.03	<0.04	<0.04	1.22	0.10	99.61	0.00	Soda-lime
	SA P5	pale purple-pink	68.83	18.44	5.96	2.25	0.55	0.65	0.53	0.10	0.58	0.07	0.23	1.09	<0.03	<0.04	<0.04	0.47	<0.06	99.75	0.00	Soda-lime
	SA P6	dark purple	65.12	18.68	6.38	2.65	0.52	1.04	1.35	0.36	2.15	0.07	0.18	0.96	<0.03	<0.04	<0.04	<0.03	0.19	99.65	0.00	Soda-lime
	SA R4	purple	67.66	19.22	6.32	2.19	0.43	0.75	0.69	0.11	1.30	0.05	0.22	1.15	<0.03	<0.04	<0.04	0.07	<0.06	100.14	0.00	Soda-lime
Green	SA VCh1	pale green	62.94	17.05	6.18	2.44	0.46	0.93	1.01	0.30	1.39	0.07	0.19	0.99	<0.03	0.62	0.29	0.06	5.37	100.28	0.06	Soda-lime-lead
	SA VCh2	pale green	64.59	17.97	6.32	2.30	0.44	0.88	1.05	0.30	1.43	0.05	0.20	1.03	<0.03	0.04	0.16	<0.03	2.98	99.74	0.03	Soda-lime-lead
	SA VCh3	pale green	63.34	18.11	6.67	2.56	0.43	1.02	1.26	0.38	1.41	0.07	0.15	1.07	<0.03	0.33	0.11	<0.03	2.47	99.37	0.03	Soda-lime-lead
	SA VCh4	pale green	68.06	18.31	5.86	2.15	0.65	0.78	0.63	0.11	0.62	0.15	0.22	1.06	<0.03	<0.04	<0.04	0.54	0.65	99.80	0.01	Soda-lime
	SA VCh5	pale green	64.90	18.41	5.52	2.34	0.70	0.85	0.86	0.15	0.47	0.18	0.24	1.13	<0.03	2.14	0.11	0.60	1.89	100.50	0.02	Soda-lime-lead
	SA VS1	dark green	64.66	17.54	6.17	2.34	0.57	0.85	0.88	0.19	0.96	0.14	0.21	0.97	<0.03	1.25	0.13	0.24	2.16	99.25	0.02	Soda-lime-lead
	SA VS2	dark green	66.95	17.44	5.74	2.32	0.67	0.64	1.28	0.12	0.43	0.15	0.16	1.01	<0.03	1.93	0.04	0.66	0.96	100.50	0.01	Soda-lime
	SA VS3	dark green	66.16	17.04	5.90	2.34	0.71	0.63	1.29	0.11	0.49	0.20	0.21	0.94	<0.03	1.74	0.05	0.52	1.37	99.72	0.02	Soda-lime-lead

Table 2. *Cont.*

Colour Macro-Group	Sample	Colour	SiO$_2$ (wt%)	Na$_2$O (wt%)	CaO (wt%)	Al$_2$O$_3$ (wt%)	K$_2$O (wt%)	MgO (wt%)	Fe$_2$O$_3$ (wt%)	TiO$_2$ (wt%)	MnO (wt%)	P$_2$O$_5$ (wt%)	SO$_3$ (wt%)	Cl (wt%)	CoO (wt%)	CuO (wt%)	SnO$_2$ (wt%)	Sb$_2$O$_3$ (wt%)	PbO (wt%)	Total	PbO/(SiO$_2$ + Na$_2$O + CaO)	Glassy Matrix
Yellow	**SA G1**	yellow	67.65	17.10	5.93	2.12	0.43	0.49	0.42	0.09	0.23	0.06	0.22	1.08	<0.03	<0.04	<0.04	0.48	3.80	100.12	0.04	Soda-lime-lead
	SA G2	yellow	68.10	17.45	5.52	2.14	0.52	0.47	0.43	0.08	0.19	0.07	0.22	1.13	<0.03	<0.04	<0.04	0.46	3.16	99.93	0.03	Soda-lime-lead
Red/Orange	**SA A1**	orange	40.01	11.36	5.04	2.20	0.60	0.55	1.60	0.13	0.12	0.18	0.19	0.51	<0.03	5.28	1.39	0.28	30.64	100.10	0.54	Lead glass
	SA R1	dark red	60.44	15.71	6.69	2.57	1.00	1.30	3.16	0.25	0.90	0.33	0.19	0.86	<0.03	1.18	0.37	0.15	5.09	100.19	0.06	Soda-lime-lead
	SA R2	red	57.47	15.47	5.37	2.28	0.61	0.69	2.69	0.14	0.19	0.18	0.24	0.96	<0.03	0.86	0.50	0.84	10.97	99.47	0.14	Lead glass
	SA R3	red	63.67	16.96	7.16	2.17	1.42	1.99	2.00	0.20	0.69	0.87	0.22	0.81	<0.03	1.24	0.11	0.16	0.18	99.83	0.00	Soda-lime
	SA Au8 *		SiO$_2$ (wt%)	Na$_2$O (wt%)	CaO (wt%)	Al$_2$O$_3$ (wt%)	K$_2$O (wt%)	MgO (wt%)	Fe$_2$O$_3$ (wt%)	TiO$_2$ (wt%)	MnO (wt%)	P$_2$O$_5$ (wt%)	SO$_3$ (wt%)	Cl (wt%)	CoO (wt%)	CuO (wt%)	SnO$_2$ (wt%)	Sb$_2$O$_3$ (wt%)	PbO (wt%)	Total		
	SA Au8 Cartellina	*pale green*	68.78	19.08	5.98	2.10	0.38	0.64	0.47	0.11	0.85	0.07	0.15	1.29	<0.03	<0.04	<0.04	<0.03	<0.06	99.98		
	SA Au8 Supporting tessera	*pale green*	67.51	18.29	6.97	2.43	0.49	0.70	0.60	0.11	1.07	0.10	0.20	1.08	<0.03	<0.04	<0.04	<0.03	<0.06	99.68		
	SA Au9 *		SiO$_2$ (wt%)	Na$_2$O (wt%)	CaO (wt%)	Al$_2$O$_3$ (wt%)	K$_2$O (wt%)	MgO (wt%)	Fe$_2$O$_3$ (wt%)	TiO$_2$ (wt%)	MnO (wt%)	P$_2$O$_5$ (wt%)	SO$_3$ (wt%)	Cl (wt%)	CoO (wt%)	CuO (wt%)	SnO$_2$ (wt%)	Sb$_2$O$_3$ (wt%)	PbO (wt%)	Total		
	SA Au9 Cartellina	*colourless*	65.11	19.05	6.35	2.65	0.32	1.55	1.31	0.30	2.20	0.03	0.22	1.11	<0.03	<0.04	<0.04	<0.03	<0.06	100.19		
	SA Au9 Supporting tessera	*colourless*	64.87	19.03	6.37	2.59	0.32	1.53	1.33	0.30	2.23	0.06	0.19	1.03	<0.03	<0.04	<0.04	<0.03	<0.06	99.86		

To calculate the PbO/(SiO$_2$ + Na$_2$O + CaO) ratio in tesserae having the PbO content lower than the EPMA detection limit (DL) for that element (Table S1a), a value of DL/2 was used, supposing that its real value may be described by a distribution of uniform probability, between zero and DL [15].

The tesserae from *S. Agnese* were produced following the Roman/Early Medieval tradition. The low MgO* and K$_2$O* contents (both under 1.5 wt%) of the glassy matrices indicate that natron was used as a flux for all the *S. Agnese* samples, and this is in line with the production technologies of the 7th cent. AD, the date of the present mosaic. It is known, in fact, that natron is the flux adopted in glass mosaics and vessels from the Roman to Medieval times (until the 9th century AD). Neither Medieval plant ash nor modern tesserae were identified, confirming the potentiality of multispectral investigations as a preliminary tool to guide sampling towards the original pars of mosaic under study [8].

Interestingly, red tessera, SA R3, and all the opaque white tesserae from *S. Agnese* are characterised by K$_2$O* contents compatible with the use of natron as flux (K$_2$O* < 1.5 wt%) but show high MgO* contents (MgO* > 2 wt%), which set these samples apart from the natron glass area (Figure 2a and Table 3).
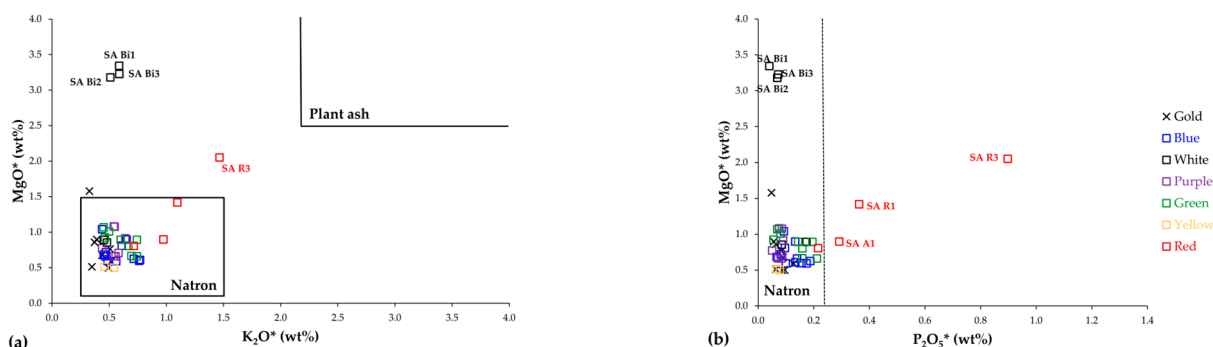
Figure 2. Binary diagrams of (**a**) MgO* vs. K$_2$O* and (**b**) MgO* vs. P$_2$O$_5$* of *S. Agnese* tesserae subdivided by colour macro-groups (EPMA data, expressed as oxide weight percentage; * refers to elements in the reduced composition). Compositional areas of glass produced by natron (in (**a**,**b**)) or plant ash (in (**a**)) were also reported.

In the case of SA R3, it should be noted that compositions that fall in the intermediate field between natron and plant ash glass are quite frequent in tesserae having red, brown, and orange colours, regardless of their dating and provenance and this evidence, being virtually absent in other coloured glass, suggests a strict technological link between colour and composition, and consequently between specific recipes and/or production techniques. The production of opaque red (including brown or orange) glass requires a locally reducing environment that can be obtained by means of several internal reducing agents, among which ashes or charcoal, as already suggested by ancient literary sources and recent analytical studies [16]. In this context, it is likely that the 'plant ash like fingerprint' identified in the red, orange and brown tesserae may be explained with the addition of plant ash during the glass-colouring rather than the glassmaking process [16]; when ash is introduced in a natron-based glass, this can generate an 'intermediate composition', like in the case of SA R3. The ash addition also generates a tendency to higher phosphorous contents in the glassy matrix, as demonstrated by other red tesserae in the *S. Agnese* assemblage, in particular SA A1 and SA R1 (Figure 2b). Having in mind that tessera SA R3 shows the highest K$_2$O* content of *S. Agnese* assemblage (Table S2), pollution from furnace ashes and charcoal due to recycling cannot be completely excluded [17], even if this leads to an increase of both potash and phosphorous contents but not of magnesia too, as in SA R3.

The interpretation of opaque white tesserae with high magnesium contents (SA Bi1, SA Bi2 and SA Bi3) is more problematic (Table 3) because they do not show any other chemical characteristics, as the high phosphorous contents of most red *S. Agnese* tesserae (Figure 2b), which could be related to glass colouring. However, this unusual composition was already observed in white tesserae, which came from other mosaics in Rome dating from the 6th to the 12th cent. AD (mosaics from *S. Lorenzo fuori le mura* and *SS. Cosma e Damiano*, 6th cent. AD; *SS. Primo e Feliciano*, 7th cent. AD; *S. Cecilia*, 9th cent. AD; *S. Clemente*, 12th cent. AD) [1]. Similar compositions were also identified in white tesserae from Padua

(mosaic of St. Prosdocimus, 6th cent. AD), Ravenna (Neonian Baptistery, 5th cent. AD, and Basilica of S. Severo, 6th cent. AD) [18], and *S. Vincenzo al Volturno* (9th cent. AD) [19] and in-floor mosaic excavated in a Late Roman villa in Noheda (Spain) [20]. In addition, high MgO, low P_2O_5, and K_2O concentrations have also been found in other kinds of artefacts, all opaque white in colour, dated to the 2nd cent. AD, such as the *giallo antico* imitation and the *cipollino rosso brecciato* imitation from the Gorga collection [21,22]. The use of a source of Sb containing Mg [23], of sand with dolomite ($CaMg(CO_3)_2$) [24] or of a silica source rich in magnesium [25] has been suggested by various scholars as a possible explanation for the high MgO values, but this remains speculation and, at the moment, the significance of the elevated magnesium in such kind of glass, all opaque white in colour, is not still well understood. In any case, the occurrence of opaque white tesserae with high magnesium in various glass mosaics spanning from the Roman to Medieval period can provide important technological information because this let us suppose that they could be re-used tesserae detached from more ancient mosaics, probably of the Roman period. This peculiar composition is a consequence of the use of specific raw materials or technological processes, still to be identified, and it was probably realised in the same production centre during the Roman period and then traded to be in use in various Roman mosaics, from which opaque white tesserae could be detached to be re-used in later mosaics.

Excluding the tesserae with anomalous compositions, the glassy matrix reduced compositions of the remaining *S. Agnese* tesserae are comparable to primary compositional groups identified in natron vessels dated to the first millennium AD: Roman-Sb, Roman-Mn, HIMT, Foy 2.1, Foy 3.2, Levantine I/Apollonia type, Levantine II/Bet Eli'ezer type, Egypt I and Egypt II [26]. This suggests technological links between these two production types and supports the hypothesis that kilns producing the base glass of tesserae were not different from those producing other types of glass. In particular, by comparing the mean compositions and standard deviation of primary natron compositional groups from Roman to Early Medieval period, as reported in Schibille [27], with *S. Agnese* assemblage, four compositional groups, named SA-Roman, SA-Foy 3.2, SA-Foy 2.1, and SA-HIMT, were here identified (Table 3) and discussed in the following paragraphs.

Group SA-Roman is the largest compositional group, composed of fifteen tesserae of the colour macro-groups: gold (3 of 9 tesserae), blue (3 of 11 t.), purple (3 of 7 t.), green (3 of 8 t.), and yellow (2 of 2 t.). It is characterised by high silica (SiO_2* = 70.35 ± 0.87 wt%), relatively low soda (Na_2O* = 17.72 ± 1.01 wt%), alumina (Al_2O_3* = 2.33 ± 0.15 wt%) and titania (TiO_2 = 0.09 ± 0.03 wt%), and comparable potash and magnesia (K_2O* = 0.61 ± 0.11 wt% and MgO* = 0.63 ± 0.11 wt%, respectively) (Table 3).

Independent of the colours of the tesserae, these chemical features are consistent with those of glass typical of the Roman period. The differences in iron contents between group SA-Roman and Roman glass, as evident from Table 3, are due to the fact the *S. Agnese* tesserae are mostly composed of intentionally coloured and opacified glass, and iron is an element involved in both opacification and colouring process, and therefore, it could be intentionally added to the glass batch with technological purposes. On the contrary, the dataset used to calculate the mean chemical composition of Roman glass is mostly composed of vessels, unintentionally coloured or decoloured, where the iron is only due to impurities of the sand used. In the case of intentionally coloured glass, as in the case of the majority of tesserae belonging to this group (12 of 15 tesserae), it is not easy to identify to which Roman reference compositional group could be ascribed the base glass of these tesserae. Roman compositional groups are typically distinguished by the presence, absence, or combination of manganese and antimony, the main decolourants of the period. However, these elements are excluded from the reduced compositions because manganese functions not only as a decolourant but also as an intentional colourant, while antimony contributes to glass opacity. Nevertheless, the primary Roman reference compositional groups also exhibit significant variations in silica, soda, lime, and alumina contents. Silica and soda contents are, generally, higher and those of lime and alumina lower in the Roman Sb-decoloured glass than Mn-decoloured glass (SiO_2: 71.4 ± 1.8 wt% vs. 69.6 ± 2.3 wt%;

Na_2O: 18.7 ± 1.3 wt% vs. 16.1 ± 1.3 wt%; CaO: 5.53 ± 0.84 wt% vs. 7.92 ± 0.76 wt% and Al_2O_3: 1.91 ± 0.21 wt% vs. 2.62 ± 0.24 wt%, in Roman-Sb and Roman-Mn decoloured groups, respectively, [27]), and these elements have intermediate contents in the Mn + Sb decoloured group [28]. Therefore, having in mind the mean contents of these elements in group SA-Roman, it is possible to hypothesise that the base glass employed in the case of *S. Agnese* tesserae with Roman compositions belongs to Mn + Sb decoloured group and, to a lesser extent, to Mn-decoloured glass group.

In addition to compositions typical of the Roman period, the tesserae of *S. Agnese* show glassy matrices with compositions comparable to Late Antique/Early Medieval compositional groups, such as SA-Foy 3.2, SA-Foy 2.1, and SA-HIMT.

Group SA-Foy 3.2 is composed of eleven tesserae, belonging to colour macro-groups gold (4 of 9 tesserae), blue (4 of 11 t.), and purple (2 of 7 t.). This group is characterised by higher soda, magnesia and titania ($Na_2O^* = 19.35 \pm 1.25$ wt%; $MgO^* = 0.71 \pm 0.11$ wt%; $TiO_2^* = 0.13 \pm 0.03$ wt%), relatively lower alumina, lime and potash ($Al_2O_3^* = 2.26 \pm 0.16$ wt%; CaO^*: 5.98 ± 1.13 wt%; $K_2O^* = 0.45 \pm 0.06$ wt%), and comparable silica and iron oxide ($SiO_2^* = 69.19 \pm 2.32$ wt%; $Fe_2O_3^* = 0.79 \pm 0.30$ wt%) with respect to SA-Roman (Table 3). This group shows compositional similarities with Group 3.2—*Série* 3.2 (also known as Foy 3.2) identified by Foy et al. [29] and HIMT2 by Foster and Jackson [30]. Foy 3.2 is dated to primarily fourth- to fifth-century AD, with a possibly even longer overall lifespan, at least until the 6th–7th century AD. Up to now, small numbers of samples of glass with this composition have been recognised among assemblages, mostly composed of vessels but also of tesserae, from the Balkans, Roman Britain, northern Italy, southern France, Turkey, and Carthage [9,14,29,31–40]. Due to compositional similarities in high silica, soda, and low lime content between Foy 3.2 glass and Sb-decoloured glass from the 1st to 4th centuries, as well as recent isotopic studies [41], Foy 3.2 can be considered a continuation of the Roman antimony tradition. This suggests that the same Egyptian glassmakers may have produced Foy 3.2, lacking an affordable antimony supply. Manganese is, in fact, the decolouriser generally identified in the Foy 3.2 glass in the place of antimony of the Roman glass and this element, although not considered in the calculation of reduced compositions, is also identified in most *S. Agnese* tesserae of this compositional group. A potential antimony shortage is further supported by the mid-fourth century shift from antimony- to tin-opacified glass in high-status objects such as wall mosaics and *opus sectile* [42].

Group SA-Foy 2.1 is composed of nine tesserae of colour macro-groups: blue (2 of 11 tesserae), white (2 of 5 t.), green (2 of 8 t.), and red (3 of 4 t.). It shows lower silica and soda ($SiO_2^* = 66.87 \pm 1.58$ wt%; $Na_2O^* = 18.79 \pm 1.27$ wt%) and higher lime, alumina, potash, magnesia, iron oxide, and titania (CaO^*: 6.88 ± 0.69 wt%; $Al_2O_3^* = 2.62 \pm 0.39$ wt%; $K_2O^* = 0.70 \pm 0.21$ wt%; $MgO^* = 0.92 \pm 0.19$ wt%; $Fe_2O_3^* = 1.68 \pm 1.04$ wt%; $TiO_2^* = 0.20 \pm 0.04$ wt%) than group SA-Foy 3.2. These compositional features are like the literature group named by Foy et al. [29] as Group 2—*Série* 2.1, here named Foy 2.1. This composition was used extensively from the 5th cent. to the first half of the 7th century AD, and has been identified in vessels and tesserae of the south of France, Spain, Italy, northern Africa, Anglo-Saxon Britain, Balkans, and Cyprus [9,14,29,32,38,43–50]. The generally higher magnesia (MgO ~ 1 wt%), lime (CaO ~ 8 wt%), alumina (Al_2O_3 ~ 2.5 wt%), iron (Fe_2O_3 ~ 1.2 wt%), and titanium oxide (TiO_2 ~ 0.15 wt%) contents of group Foy 2.1 compared with Foy 3.2 suggest two distinct primary productions, although both groups are considered of probable Egyptian provenance.

Table 3. Mean chemical compositions and standard deviations of four compositional groups identified in the *S. Agnese* assemblage and of *S. Agnese* tesserae with high Mg contents (in red). Mean chemical compositions and standard deviations of the literature compositional groups used for comparisons are also shown in italics (data from [27]). See text for further details.

S. Agnese Compositional Groups			SiO$_2$* (wt%)	Na$_2$O* (wt%)	CaO* (wt%)	Al$_2$O$_3$* (wt%)	K$_2$O* (wt%)	MgO* (wt%)	Fe$_2$O$_3$* (wt%)	TiO$_2$* (wt%)	P$_2$O$_5$* (wt%)	SO$_3$* (wt%)	Cl* (wt%)	*Literature Compositional Group*
SA-Roman	Number of samples: 15	**Mean**	**70.35**	**17.72**	**6.34**	**2.33**	**0.61**	**0.63**	**0.78**	**0.09**	**0.13**	**0.22**	**0.96**	
		St. Dev.	0.87	1.01	0.52	0.15	0.11	0.11	0.39	0.03	0.05	0.05	0.19	
	Date: 1st–3st cent. AD	*Mean*	*70.50*	*17.40*	*6.73*	*2.27*	*0.55*	*0.48*	*0.38*	*0.07*	*0.09*	*n.r.*	*1.17*	*Roman*
		St. Dev.	*1.27*	*1.84*	*1.69*	*0.50*	*0.14*	*0.09*	*0.03*	*0.01*	*0.06*	*n.r.*	*0.09*	
SA-Foy 3.2	Number of samples: 11	**Mean**	**69.19**	**19.35**	**5.98**	**2.26**	**0.45**	**0.71**	**0.79**	**0.13**	**0.08**	**0.21**	**1.18**	
		St. Dev.	2.32	1.25	1.13	0.16	0.06	0.11	0.30	0.03	0.03	0.05	0.07	
	Date: 4th–7th cent. AD	*Mean*	*68.45*	*19.35*	*6.31*	*2.10*	*0.53*	*0.70*	*0.70*	*0.11*	*0.05*	*n.r.*	*1.23*	*Foy 3.2/HIMT 2*
		St. Dev.	*0.49*	*0.49*	*0.43*	*0.22*	*0.08*	*0.08*	*0.03*	*0.01*	*0.00*	*n.r.*	*0.24*	
SA-Foy 2.1	Number of samples: 9	**Mean**	**66.87**	**18.79**	**6.88**	**2.62**	**0.70**	**0.92**	**1.68**	**0.20**	**0.19**	**0.24**	**1.09**	
		St. Dev.	1.58	1.27	0.69	0.39	0.21	0.19	1.04	0.04	0.09	0.04	0.16	
	Date: 4th–7th cent. AD	*Mean*	*65.70*	*17.70*	*8.12*	*2.53*	*0.75*	*1.12*	*1.16*	*0.15*	*0.16*	*n.r.*	*0.83*	*Foy 2.1*
		St. Dev.	*1.70*	*1.30*	*0.92*	*0.23*	*0.19*	*0.25*	*0.50*	*0.02*	*0.10*	*n.r.*	*0.11*	
SA-HIMT	Number of samples: 7	**Mean**	**67.27**	**18.96**	**6.66**	**2.63**	**0.47**	**1.11**	**1.32**	**0.34**	**0.07**	**0.19**	**1.06**	
		St. Dev.	0.72	0.32	0.15	0.11	0.07	0.21	0.19	0.05	0.02	0.02	0.04	
	Date: 4th–7th cent. AD	*Mean*	*66.70*	*18.80*	*6.06*	*2.64*	*0.47*	*1.00*	*1.51*	*0.38*	*0.05*	*n.r.*	*1.01*	*HIMT*
		St. Dev.	*1.80*	*1.20*	*0.63*	*0.34*	*0.11*	*0.16*	*0.37*	*0.13*	*0.02*	*n.r.*	*0.09*	
Opaque white—high Mg	Number of samples: 3	**Mean**	**69.15**	**17.69**	**5.74**	**2.18**	**0.56**	**3.23**	**0.51**	**0.06**	**0.06**	**0.69**	**0.29**	
		St. Dev.	0.74	0.72	0.15	0.08	0.04	0.08	0.03	0.00	0.02	0.02	0.02	
Red— high Mg and P	Number of samples: 1	**SA R3**	**65.25**	**17.38**	**7.34**	**2.22**	**1.45**	**2.03**	**2.05**	**0.20**	**0.89**	**0.23**	**0.83**	

Asterisk refers to elements in their reduced composition, only in the case of *S. Agnese* compositional groups and of *S. Agnese* tesserae with high Mg; n.r.: not reported.

Finally, **group SA-HIMT** comprises seven tesserae of the colour macro-groups: gold (1 of 9 tesserae), blue (1 of 11), purple (2 of 7 t.), and green (3 of 8 t.). This group is characterised by high iron oxide, titania and magnesia (Fe_2O_3* = 1.32 ± 0.19 wt%; TiO_2* = 0.34 ± 0.05 wt%; MgO* = 1.11 ± 0.21 wt%), in particular that of titania is the highest of the whole assemblage, and comparable silica, soda, lime and alumina contents (SiO_2* = 67.27 ± 0.72 wt%; Na_2O* = 18.96 ± 0.32 wt%; CaO*: 6.66 ± 0.15 wt%; Al_2O_3* = 2.63 ± 0.11 wt%) with those of group SA-Foy 2.1. Although not considered in the reduced composition, it is worth noting the high manganese content of the base glass of SA-HIMT tesserae (MnO = 1.64 ± 0.55 wt%). As reported by Schibille [27], this glass composition with elevated iron, titanium, and manganese oxide concentrations, designated as HIMT (High-Iron Manganese Titanium) by Freestone [51], appeared in the archaeological record of the fourth century AD. HIMT is a very common type of glass identified throughout the Mediterranean (except the Levant) as well as in central and northern Europe, produced and traded mostly between the 4th and 5th cent. AD, even if this composition is attested until the 7th cent. AD [38–40,43,52,53]. The exceptionally high iron, manganese, and heavy elements concentrations, which are the distinctive features of HIMT glass, are due, in part, to the Nilotic sands used as raw materials, in part to manganiferous materials added for decolouring purposes [52,53], and this, together with results of some isotopic analyses, suggests an Egyptian provenance also for this glass composition [27], in addition to groups Foy 3.2 and Foy 2.1.

4.2. Opacifiers/Pigments and Other Crystalline Inclusions

A prevalence of antimony-based opacifiers, both Ca-antimonate and Pb-antimonate, typical of Roman tradition, was identified in the tesserae of *S. Agnese fuori le mura*, but tin-based (cassiterite and Pb-stannate) and copper-based opacifiers (metallic copper and cuprite) were also present.

Ca-antimonate, which is a white opacifier, was identified in all white, blue, and in most of the opaque purple tesserae in *S. Agnese* (four over seven opaque purple tesserae, e.g., SA P1, SA P3, SA P4 and SA P5). The remaining purple ones are translucent without any opacifiers, and one has other opacifiers, as detailed in the following paragraphs.

The density of Ca-antimonate particles within the glass matrix varies and correlates with colour, influencing the tesserae's opacity. White tesserae and most blue tesserae (except for SA B3, SA B4, SA B5, and SA B8), along with purple tesserae SA P1 and SA P4, exhibit high Ca-antimonate concentrations (Figure 3a), resulting in complete opacity. Conversely, blue tesserae SA B3, SA B4, SA B5, SA B8, and purple tesserae SA P3 and SA P5 contain sporadic Ca-antimonate (Figure 3b), leading to semi-opacity. Ca-antimonate micro-texture reveals a relatively uniform distribution of geometric crystals (approximately 5–10 μm) dispersed within the homogenous glass matrix. They are found as isolated crystals, as aggregates of crystals with euhedral habit, or as aggregates of small crystals with various shapes and sizes (Figure 3c,d), the so-called rosary-shaped aggregations (Figure 3e).

The euhedral habit of Ca-antimonate crystals, identified in all the white, blue (except for turquoise), and purple tesserae SA P1 and SA P4, suggests in situ crystallisation, i.e., the crystals precipitated directly from the soda-lime glass melt. This is considered the most common opacification process for this kind of opacifier [54].

The Ca-antimonate identified into turquoise tesserae is composed of rosary-shaped aggregates, suggesting that the ex-situ method was used. This implies that calcium antimonate opacifiers were first synthesised and then added to the molten glass [55,56].

XRPD analyses gave diffraction patterns on the samples with Ca-antimonate identified using SEM-EDS, except in blue SAB3, SAB4, SA B5, and SA B8 and in purple SAP3 and SAP5, due to the low concentration of inclusions. These analyses allow us to identify which kind of Ca-antimonate is present in each tessera, keeping in mind that this phase shows two modifications, hexagonal ($CaSb_2O_6$) and rhombic ($Ca_2Sb_2O_7$), related to different firing times and temperatures [57].
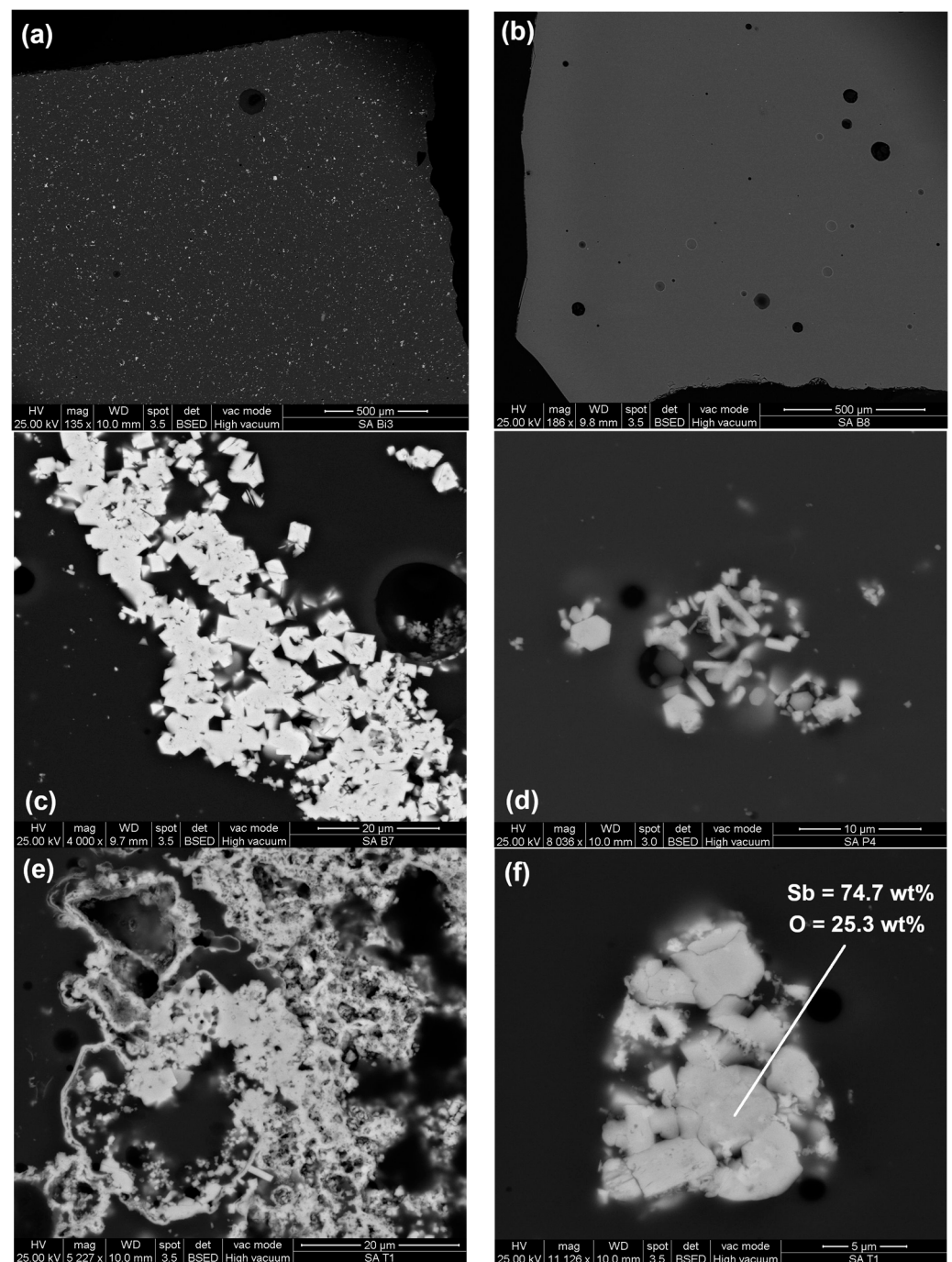
Figure 3. SEM-BSE images of tesserae with Ca-antimonate: (**a**) micro-texture of opaque white tessera SA Bi3 with high concentrations of Ca-antimonate; (**b**) micro-texture of semi-opaque blue tessera SA B8 with the sporadic presence of opacifiers; (**c**,**d**) details of Ca-antimonate crystals with euhedral habit in opaque blue SA B7 and opaque purple SA P4, respectively; (**e**) detail of Ca-antimonate rosary-shaped aggregates in opaque turquoise SA Tu1; (**f**) relict of antimony oxide in opaque turquoise SA Tu1. SEM-EDS data are also shown in (**f**).

In all the blue tesserae from *S. Agnese*, except for SA B7, only rhombic $Ca_2Sb_2O_7$ was identified, while in the purple, only the hexagonal $CaSb_2O_6$ was detected. In tessera SA B7 and all-white ones, both phases are present. The presence of both phases in *S. Agnese* white tesserae, having high Mg in the glassy matrix, seems to contradict the preliminary hypothesis that Mg has a favourable impact on the formation of only rhombic Ca-antimonate [58], but further investigations are required to confirm this trend. In any case, in *S. Agnese*

tesserae, in which in situ crystallisation was hypothesised (e.g., all with Ca-antimonate, except for the turquoise ones), the presence of both phases in white SA Bi1, SA Bi2, SA Bi3, and in blue SA B7 suggests a firing duration of 1–2 days at approximately 1100 °C. Conversely, the presence of solely the hexagonal phase in purple tesserae (SA P1, SA P4) indicates shorter firing times (less than a day) at higher temperatures (above 1100 °C). Blue samples SA B1, SA B2, SA B6, and SA B9, containing only the rhombic phase, were likely produced with longer firing times (over two days) at lower temperatures (<1100 °C). However, as recently documented in an experimental study carried out by Boschetti et al. [58], temperatures lower than 1100 °C for the precipitation of Ca-antimonate, independently from the phase symmetry, can also be hypothesised in glass tesserae showing a very low quantity of lead in the glassy matrix, as in the case of all blue *S. Agnese* tesserae, except for SA B5.

In the case of turquoise tesserae, in which ex situ crystallisation of Ca-antimonate is hypothesised by the micro-textural point of view, it is interesting to note that only rhombic $Ca_2Sb_2O_7$ was identified. This is in accordance with studies by Lahlil et al. [56] on Egyptian opaque white, blue and turquoise glass, where ex situ crystallisation is documented. They proposed that Egyptian artisans created $Ca_2Sb_2O_7$ by heating mixtures of Sb_2O_3 or Sb_2O_5 with calcium carbonates between 1000 and 1100 °C. Supporting this production technology is also the finding of antimony oxide in both turquoise samples (Figure 3f), likely a remnant of the antimony source material.

As in *S. Agnese* mosaic, both in situ and ex situ crystallisation methods of Ca-antimonate were already identified in other Roman and Early Medieval tesserae from North-eastern Italy, such as, for example, those of St. Prosdocimus in Padua [50], those from Pordenone and Trento [59], those from the "Casa delle Bestie Ferite" in Aquileia [60] and those from the monastery of San Severo in Classe (Ravenna) [61].

Furthermore, in blue tesserae SA B3, SA B4, SA B5, and SA B8 and the purple ones SA P3 and SA P5 (all semi-opaque), rare Ca-antimonates are found in association with very abundant gas bubbles and, only in the case of purple tesserae by quartz and terracotta grains, suggesting that gas bubbles were intentionally produced and other opacifiers were added to increase the opacity degree of these tesserae, and only in the case of terracotta grains, to influence the final colour, as detailed in the following paragraphs.

Ca-antimonate, as opacifier/pigment, was documented in the majority of glass mosaics in Rome from the 5th to the 13th cent. AD [1], suggesting that in mosaics from Rome, the use of Ca-antimonate goes beyond the Late Antique period, even if the strong recourse of recycling and/or re-use of Roman tesserae cannot be completely excluded, and further studies are necessary to clarify this point.

Pb-antimonate, used as opacifier/pigment being yellow in colour, was identified in all opaque yellow and in 4 (of 8) opaque green tesserae from *S. Agnese* (two pale green—SA VCh4 and SA VCh5—and two dark green—SA VS2 and SA VS3).

The micro-texture of the tesserae differs in the various colours. In the case of opaque green tesserae (both pale and dark green), the micro-texture is homogeneous (Figure 4a), with crystals of opacifiers generally distributed through the glassy matrix. In contrast, opaque yellow tesserae display an inhomogeneous matrix with distinct zones visible in the BSE images due to varying heavy element contents—lead in particular (Figure 4b). Independently from the different micro-textures, opacifiers form aggregates of various shapes and sizes composed of compactly arranged crystals with different morphologies. Some exhibit regular cubic crystals, with a mean size of 10 μm (Figure 4c), while others consist of very small granular crystals, often clustered in lumps, with anhedral habit (Figure 4d). These opacifiers primarily contain Pb and Sb, with diffraction patterns consistent with a cubic pyrochlore structure resembling the mineral bindheimite ($Pb_2Sb_2O_7$). However, SEM-EDS analyses reveal heterogeneous compositions of opacifiers, independently of their morphology, both between and within *S. Agnese* tesserae. Additionally, iron, sometimes combined with tin (samples SA G2 and SA VS3), is mostly present in lead antimonate aggregates in the *S. Agnese* tesserae (up to 5 wt%, as Fe_2O_3—SEM-EDS data).
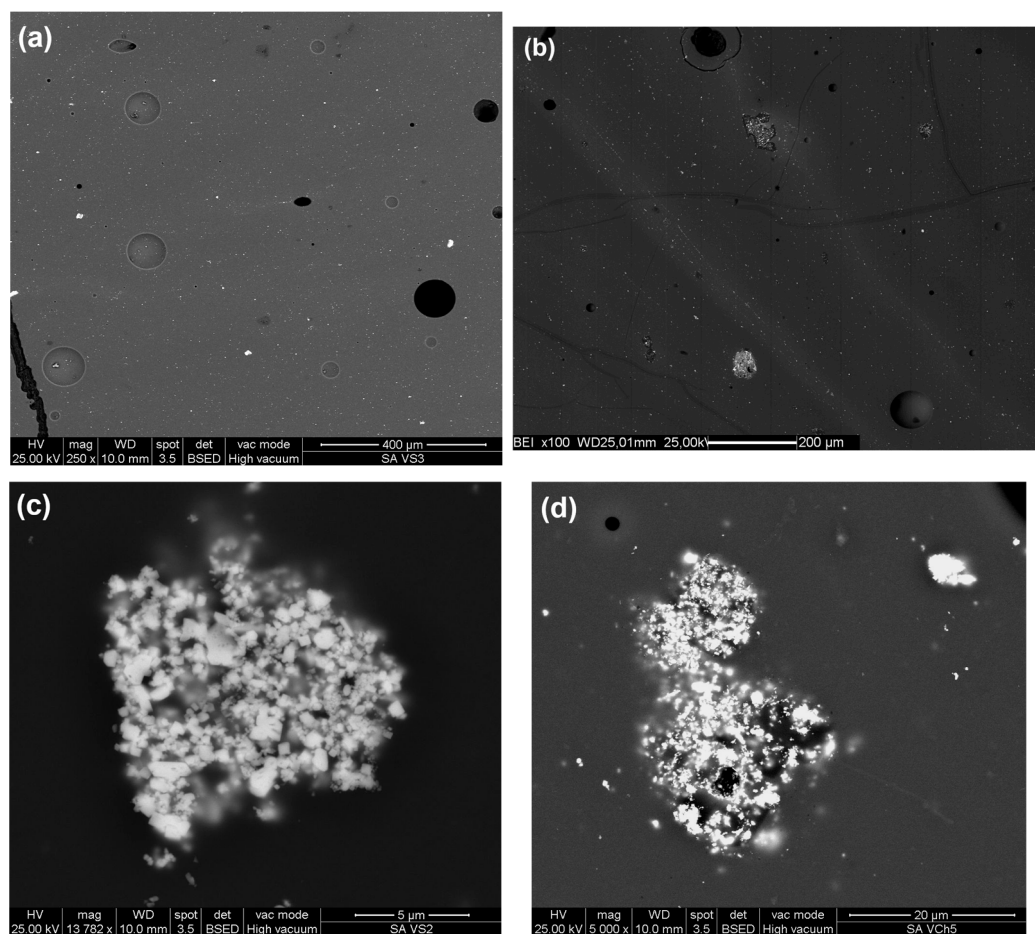
Figure 4. SEM-BSE images of tesserae with Pb-antimonate: (**a**) homogeneous micro-texture in opaque dark green tessera SA VS3; (**b**) inhomogeneous micro-texture in opaque yellow tessera SA G2; (**c**) detail of euhedral crystals, cubic in habit, in opaque dark green tessera SA VS2; (**d**) details of very small anhedral crystals, clustered in lumps, in opaque pale green tessera SA VCh5.

The prevailing hypothesis posits the ex situ synthesis of lead antimonate crystals followed by their addition to transparent glass for opacification [61,62]. This is supported by evidence of partial dissolution and clustered lead antimonate distribution [63], with small euhedral crystals forming upon cooling after partial dissolution [64]. These micro-textural features were also identified in *S. Agnese* tesserae with Pb-antimonate, further supporting the ex situ crystallisation method. The systematically very low antimony content in the glassy matrix (<1 wt% as Sb_2O_3—Table 2) is inconsistent with in situ opacifier formation. As lead antimonate can be synthesised in the air at temperatures between 730 and 1000 °C [64], these temperatures were likely achieved during *S. Agnese* tesserae production, with the above phase as an opacifier.

In addition, in tessera SA VCh5, some crystals of newly formed wollastonite ($CaSiO_3$), acicular in habit, were also identified together with terracotta grains, rosary-shaped Ca-antimonate and anhedral crystals of cassiterite (SnO_2). The occurrence of different inclusions in the same sample may be explained by the recycling of opaque glass and/or the importation of opaque ingots.

Pb-antimonate was documented in the green and yellow tesserae from all 5th–9th cent. AD mosaics from Rome, except for the *S. Pudenziana* mosaic, where such colours were not analysed. In detail, Pb-antimonate was identified in *S. Sabina* (5th cent. AD), *S. Teodoro al Palatino* (second half of 6th cent. AD), *SS. Cosma e Damiano* (6th cent. AD), *S. Lorenzo fuori le mura* (6th cent. AD), *SS. Primo e Feliciano* (7th cent. AD), *S. Pietro in Vincoli* (7th cent. AD), and *S. Cecilia* (9th cent. AD) [1].

Tin-based opacifiers (Pb-stannate and cassiterite), typical of the Late Antique/Early Medieval period, are also identified in *S. Agnese fuori le mura*. In particular, Pb-stannate, a yellow pigment, was identified in four (of eight) opaque green tesserae in *S. Agnese* (three pale green—SA VCh1, SA VCh2, and SA VCh3—and one dark green—SA VS1), while cassiterite (SnO_2), a white pigment, was identified in all opaque grey tesserae of *S. Agnese* (SA Gr1 and SA Gr2).

Tesserae opacified with Pb-stannate exhibit an inhomogeneous micro-texture due to the uneven lead distribution within the glassy matrix, creating distinct bands well visible in the SEM-BSE image: the bands having higher lead appear lighter grey than those with lower lead, which are darker grey in colour (Figure 5a). Pb-stannate appears as pseudo-cubic, newly formed crystals, with a mean size of about 3 μm, often associated with newly formed acicular cassiterite crystals (Figure 5b). The opacifier is mainly composed of Pb and Sn, with diffraction patterns consistent with cubic $PbSnO_3$. However, SEM-EDS analyses often show silicon, in addition to lead and tin (Figure 5b), letting us suppose that the opacifier is composed of cubic $PbSn_{1-x}Si_xO_3$, also defined as lead–tin-oxide type II [65], as already hypothesised, for instance, in green and yellow tesserae from the St. Prosdocimus mosaic in Padua [14]. This opacifier can be produced by heating a mixture of PbO and SnO_2 with silicon dioxide (SiO_2) at 700–900 °C in air. Heating PbO and SnO_2 without SiO_2 yields, not chromophorous tetragonal lead tin oxide (Pb_2SnO_4). In addition, it was experimentally verified that lead–tin-oxide type II crystals are stable at up to 750 °C–1000 °C, decomposing and recrystallising as SnO_2 at higher temperatures [65].
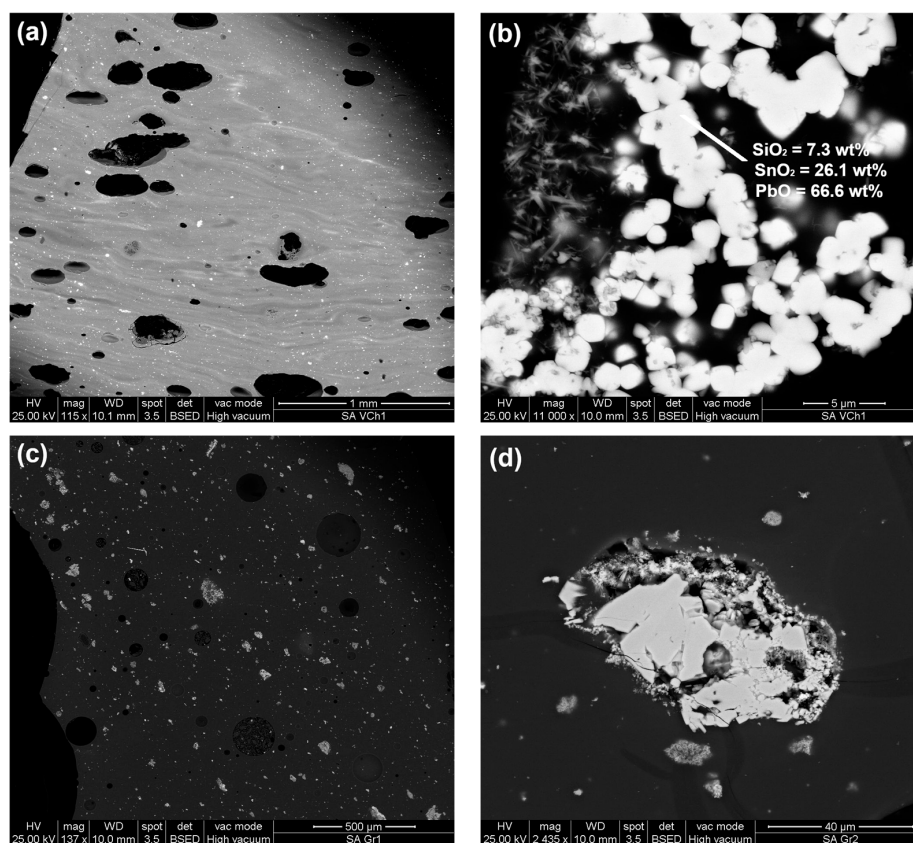
Figure 5. SEM-BSE images of tesserae with Sn-based opacifiers: (**a**) banded micro-texture of opaque pale green tessera SA VCh1, having Pb-stannate as main opacifier; (**b**) detail of pseudo-cubic crystals, composed of Pb-stannate associated with newly formed acicular crystals of cassiterite in SA VCh1; (**c**) homogeneous micro-texture of opaque grey tessera SA Gr1, having cassiterite as main opacifier; (**d**) details of anhedral crystals of cassiterite in opaque grey tessera SA Gr2. SEM-EDS data are also shown in (**b**).

Tesserae opacified with cassiterite shows a homogenous micro-texture, and the opacifier is well dispersed throughout the glass (Figure 5c). It is generally found in aggregates of various shapes and sizes, and most of crystals have anhedral habit (Figure 5d).

The micro-textural, chemical and mineralogical evidence suggests that, in the *S. Agnese* samples, the $PbSnO_3$ pigment was produced separately and added to soda-lime glass, while SnO_2 was likely added directly to translucent glass by crushing the mineral cassiterite. The non-uniform micro-texture in tesserae with Pb-stannate (Figure 5a), in fact, may indicate rapid, low-temperature, and poor opacifier mixing to prevent lead stannate transformation into cassiterite. To further investigate the production process of tin-based opacified tesserae, PbO/SnO_2 and PbO/SiO_2 ratios were examined. Following Tite et al. [42] and Matin et al. [65], in the case of synthesis ex situ of tin-based opacifiers, when the PbO/SiO_2 ratio is fixed, samples with a high PbO/SnO_2 ratio should exhibit the coexistence of $PbSnO_3$ and SnO_2, the last arising from the initial dissolution of lead stannate at temperatures between 860 °C and 930 °C. Conversely, a low PbO/SnO_2 ratio should favour the formation of lead stannate, inhibiting the recrystallisation of cassiterite, which starts from 1040 °C onwards. Based on these considerations and fixed the PbO/SiO_2 ratio to about 0.05 for all *S. Agnese* tesserae with Sn-containing opacifiers, the tesserae SA VCh1, SA VCh2, SA VCh3, and SA VS1, which show high PbO/SnO_2 (about 19%), should contain $PbSnO_3$ together with minor cassiterite, and this was experimentally verified. *S. Agnese* tesserae SA Gr1 and SA Gr2 with low PbO/SnO_2 (about 1.7) should have only Pb-stannate and not cassiterite as an opacifier, but they experimentally show only cassiterite and not Pb-stannate.

Therefore, the above analytical evidence, together with the anhedral opacifier habit, supports the hypothesis of ex situ cassiterite crystallisation. The low lead content in the glassy matrix (2.15 ± 0.7 wt% as PbO; Table 2) of cassiterite-containing *S. Agnese* tesserae is also inconsistent with in situ opacifier crystallisation. The homogeneous micro-texture of these tesserae suggests prolonged, effective opacifier mixing in the molten transparent glass, preventing cassiterite transformation due to its low solubility.

Tin-based opacifiers were documented in few Roman mosaics. Pb-stannate was, in fact, identified only in *SS. Cosma e Damiano*, *S. Sabina*, and *S. Cecilia* mosaics, while cassiterite, as the only opacifier, was identified so far in mosaics dated to the 13th cent. AD, such as those of *S. Maria in Trastevere* and *S. Cecilia-Ciborio* [1]. Therefore, the occurrence of such type of opacifier in a glass mosaic dates back to the 7th cent. AD is particularly significant because it testifies that cassiterite, together with lead-stannate, is also attested as the main opacifier in Early Medieval mosaics in Rome.

Other opacifiers, not related to a specific historical period, were also identified in *S. Agnese* tesserae. These are the **copper-based opacifiers, i.e., metallic copper and cuprite**. In particular, metallic copper was identified in all opaque red tesserae from *S. Agnese*, while cuprite, coupled with sporadic metallic copper, was identified in only one orange tessera from *S. Agnese*.

The opacity and colour in all opaque red tesserae (SA R1, SA R2, SA R3) result from abundant metallic copper particles. These particles precipitated as cubic euhedral crystals within the molten glass, reaching an average size of a few hundred nanometers (Figure 6a). In the red tesserae from *S. Agnese*, different colour bands (darker and lighter red) are also well visible to the naked eye, and microscopically, these colour variations correspond to differences in copper crystal size. The copper crystals are, in fact, smaller in the light red areas and larger in the dark red ones, and the different dimensions of the copper crystals follow the macroscopic colour zoning disposed in horizontal bands (Figure 6b).
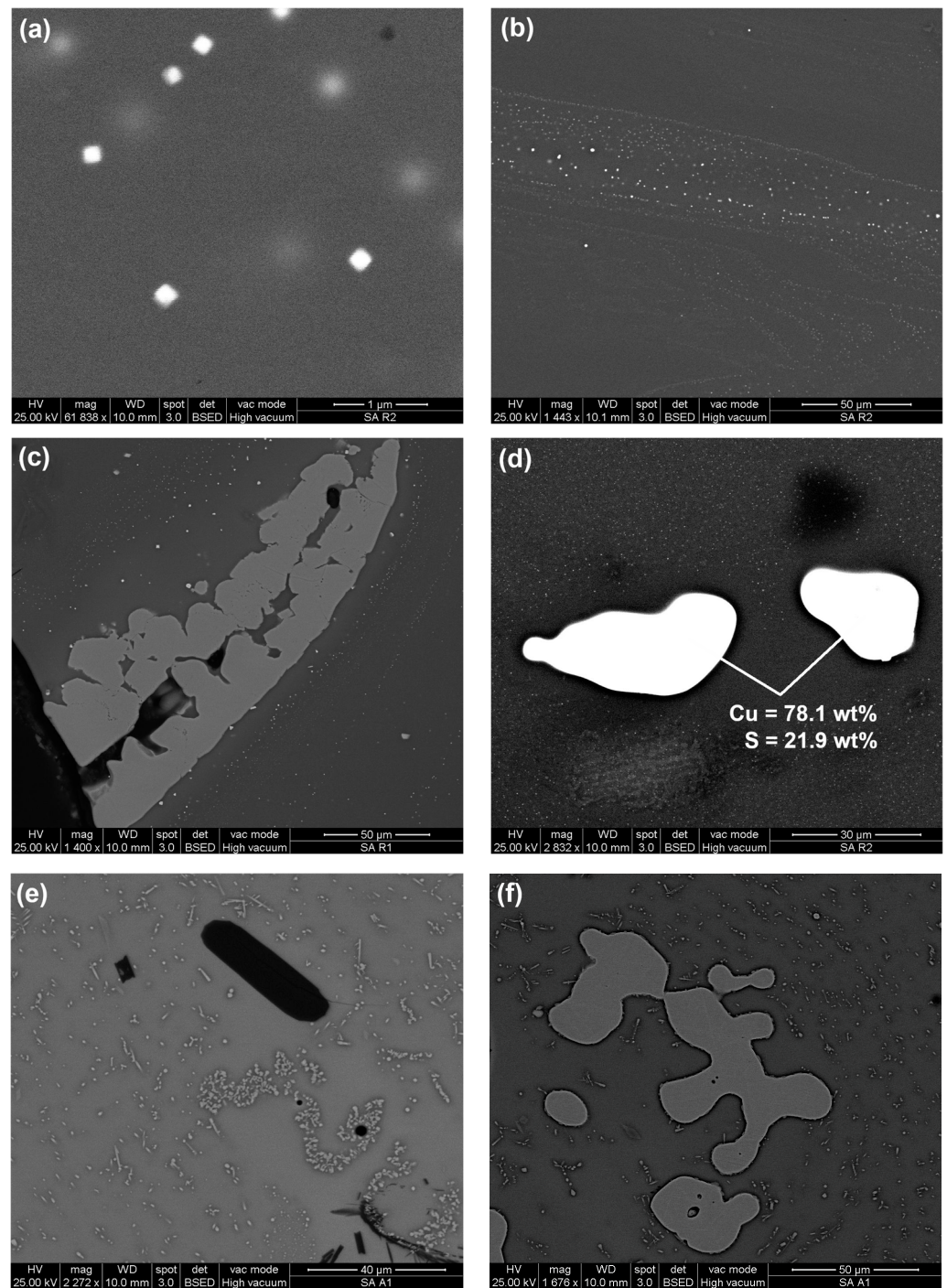
Figure 6. SEM-BSE images of tesserae with Cu-based opacifiers: (**a**) nanometric cubic crystals of metallic copper in opaque red tessera SA R2; (**b**) different dimensions of metallic copper crystals, macroscopically related to different colours bands, in opaque red tessera SA R3; (**c**) detail of inclusion composed of metallic iron surrounded by nanometric metallic copper in opaque red tessera SA R1; (**d**) detail of copper sulfide inclusions in SA R2; (**e**) cuprite crystals, having cubic and dendritic morphology, coupled with newly formed crystals of wollastonite (black in colour); (**f**) details of sporadic cluster composed of metallic copper, surrounding by cuprite micro-crystals. SEM-EDS data are also shown in (**d**).

In general, colour generation in red glass is a complex process that generally requires excess copper and reducing conditions, while lead presence is not essential to the precipitation of metallic copper [16,66]. This trend is also confirmed in three *S. Agnese* red tesserae,

which all show copper in the glassy matrix (CuO about 1 wt%, Table 2) and variable lead (PbO: from negligible in SA R3 to about 11 wt% in SA R2, Table 2).

The batch composition, related to other elements, also cooperates in the colouring process, thanks to the addition of reducing agents (such as Fe, Sb, and Sn), which contribute to the precipitation of metallic copper [16,66,67]. All the *S. Agnese* red tesserae show very high iron (Fe$_2$O$_3$: 2–3 wt%, Table 2) coupled with variable tin and antimony contents (both lower in SA R3 and higher in SA R2—SnO$_2$: 0.11 and 0.50 wt%; Sb$_2$O$_3$: 0.16 and 0.84 wt%, respectively; and intermediate tin and low antimony in SA R1—SnO$_2$: 0.37 and Sb$_2$O$_3$: 0.15 wt%, Table 2). Interesting to note that tessera SA R3 is always characterised by abundant metallic copper as opacifier/pigment, notwithstanding it has the lowest contents of iron, tin, antimony, and lead (Table 2). In this case, as already discussed in Section 4.1, the probable reducing agent is plant ash, added during glass colouring.

The micro-textural and chemical examinations, carried out using SEM analyses, of the three red tesserae from *S. Agnese* yield further insights into their production technology. In tessera SA R1, an inclusion composed of metallic iron surrounded by metallic copper crystals was identified (Figure 6c), suggesting that metal scraps were used as a source of one of the reducing agents. On the contrary, the occurrence of metallic copper associated with copper sulfide (Cu:S = 80:20 chalcocite, a possible relic of copper ore) in tesserae SA R1 and SA R2 (Figure 6d) indicates that the source of copper is from ore rather than metal scraps.

In only one orange tessera from *S. Agnese* (SA A1), the colour and opacity are due to cuprite, confirmed by XRPD analyses. At SEM, cuprite shows cubic habit, with a mean size of about 100 nm, homogeneously distributed in the glassy matrix, although this phase was also locally found aggregated into dendritic morphology (Figure 6e). Sporadic occurrence of metallic copper clusters was also identified in that area, where the tessera macroscopically appears more reddish in colour (Figure 6f). The orange tessera is characterised by very high lead and copper (PbO and CuO: 30.64 and 5.28, respectively, Table 2), confirming that the precipitation of this crystalline phase is stimulated by lead.

Notwithstanding in the literature it is reported that a high lead content in glassy matrix reduces the precipitation of devitrification phases composed of xNa$_2$O-yCaO-zSiO$_2$ crystals (mainly combeite, wollastonite, but also pyroxenes) (e.g., [68]), this is not verified in the *S. Agnese* orange tessera, where numerous newly formed crystals of wollastonite were identified (Figure 6e). The same is also documented in orange tesserae from other Italian sites (e.g., [16]).

Other reducing agents, such as iron, tin, and antimony, were also detected in the glassy matrix of the *S. Agnese* orange tessera. The association of copper and tin and the absence of other phases, which can suggest a link with the copper ores, let us hypothesise that in this case, a tin bronze was introduced in the batch as a source of copper, as documented in other orange tesserae with comparable dating from Italy (e.g., [16], and, more in general, in translucent glass coloured by means of copper.

Copper-based opacifiers were also identified in all the orange and red tesserae from other mosaics from Rome, dating from the 6th to the 13th cent. AD (*S. Teodoro*, *S. Lorenzo*, *SS. Cosma e Damiano*, *SS. Primo e Feliciano*, *S. Pietro in Vincoli*, *S. Cecilia*, *S. Clemente*, *S. Maria Nova* and *S. Maria in Trastevere*), having glassy matrices produced by using both natron and soda plant ash as flux [25]. Having in mind that these types of opacifiers are also diffused in red Prehistoric and Roman glass [69], this evidence further confirmed that the use of this kind of copper-based opacifiers/pigments is not related to a specific historical period, but they were used throughout the whole glass history for colouring and opacifying glass in red/orange/brown hues. The common trend between the *S. Agnese* red and orange tesserae and those from the other mosaics from Rome is that orange tesserae are always characterised by very high lead contents, while the red tesserae show variable lead contents, from negligible to high, although those with medium-high lead are in prevalence. Interesting to note that while in the orange tesserae, the opacifier is always composed of

cuprite, in the red tesserae from other Roman mosaics, both the only metallic copper and the association of metallic copper and cuprite are detected in the red tesserae.

Grains of terracotta, identified in association with other opacifiers/pigments and not related to a specific colour, were also attested in *S. Agnese fuori le mura* tesserae. In particular, terracotta was identified into all the yellow tesserae, the majority of opaque green tesserae (six of eight tesserae, four pale green Sa VCh1, SA VCh2, SA VCh4, and SA VCh5 and 2 dark green SA VS1 and SA VS2) and in two of five opaque purple tesserae (SA P3 and SA P5) (Figure 7a).
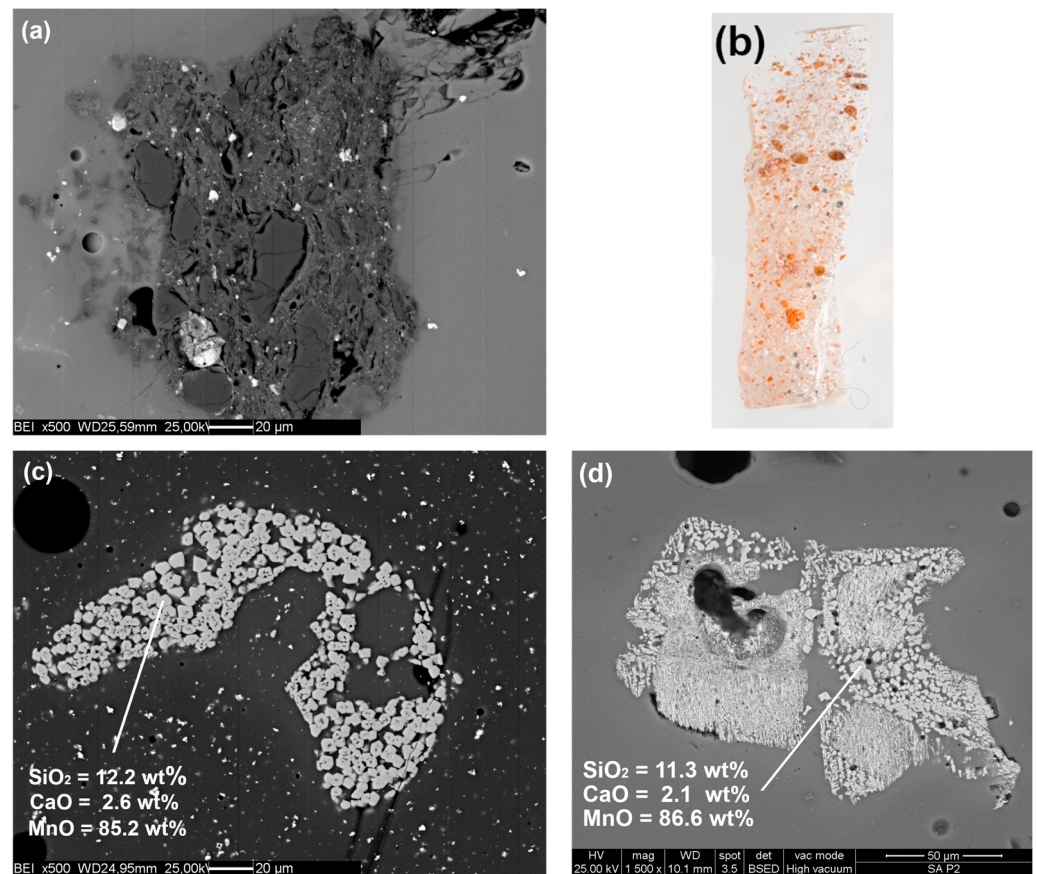
Figure 7. SEM-BSE and OM-st images of other types of inclusions identified in *S. Agnese* tesserae: (**a**) terracotta grains in opaque pale pink-purple tessera SA P3 (SEM-BSE image); (**b**) reddish inclusions composed of terracotta grains in SA P3 (OM-st image); (**c**,**d**) details of Mn-inclusions in opaque purple tesserae SA P1 and SA P2 (SEM-BSE images). SEM-EDS data are also shown in (**c**,**d**).

Terracotta grains were documented in most glass mosaics from Rome [1], in particular in the tesserae used for the skin of the people, in accordance with that reported in the Montpellier recipe book [70], but this type of opacifier is generally uncommon in glass mosaics from other sites. Terracotta is an economic opacifier, and, probably, it was used to ample the palette of colours available to mosaic-makers. However, its addition to the batch would create technological problems due to the different thermal properties between this material and the glass. This problem was solved by glassmakers by using grains with specific dimensions—not too big, to reduce the stress between glass and grain during cooling, and not too small, to avoid their dissolution in the glass and, therefore, possible changes in the final colour of tessera [25]. A generally uniform dimension of terracotta grains (mean dimensions between 50 and 150 μm) in diameter is also evident in *S. Agnese* tesserae (Figure 7a), confirming the adoption of this technological solution.

In the two purple tesserae (SA P3 and SA P5), terracotta grains were the prevalent opacifiers, but they were coupled with many gas bubbles, quartz, and a few Ca-antimonate

crystals. This is probably due to an intentional technological choice, aiming to realise pink tesserae, semi-opaque in appearance, by means of the combination of red hue due to many terracotta grains and the white hue due to the Ca-antimonate and quartz mixed in a naturally coloured glass (Figure 7b). The process demonstrates specific attention to the opacity and the chromatic result of tesserae used for the flesh tones, which is remarkable considering the singular choice to make the saint's face with stone tesserae [71].

Finally, in three purple tesserae from *S. Agnese* SA P1, SA P2, and SA P6, **Mn-containing inclusions** were also identified. The inclusions, which at SEM are brighter than glassy matrix, are characterised by aggregates of micro-crystals, euhedral in habit and with diameters generally <10 μm each, even if more acicular crystals are also detected. Independently from morphology, inclusions are all chemically composed of manganese, silicon, and calcium in similar ratios (Figure 7c,d).

The micro-texture of the crystals suggest that they are new-formed phases, precipitated into the glassy matrix, but they cannot be considered as opacifiers or pigments. These inclusions, which are quite sporadic, in fact, coexist with other most abundant opacifiers, such as Ca-antimonate in SA P1 and cassiterite in SA P2; while their quantity is not sufficient to opacify glass in SA P6, which is a translucent tessera.

In any case, the finding of such Mn-inclusions is here underlined because similar crystals to those of *S. Agnese* (both in micro-texture and chemistry) were already identified in other EarlyMedieval glass tesserae from Padua [72], and they revealed as useful technological markers to constrain melting temperature. If, in fact, the Mn-containing inclusions found in Rome tesserae are of the same type as those identified in Padua tesserae (e.g., a Ca-rich braunite, as the chemistry and micro-texture seem to confirm), it is possible to hypothesis that melting temperatures ranging from 1000 °C to 1150 °C, were reached in the production of *S. Agnese* tesserae. In addition, as in the case of Paduan tesserae, it is remarkable to note that the same phase is identified in tesserae, characterised by different glassy matrices and opacifiers. In particular, glassy matrices of SA P2 and SA P6 show good chemical comparability with the HIMT group, while SA P1 is similar to Roman glass; SA P1 and SA P2 show Ca-antimonate and cassiterite as opacifiers, respectively.

The comparability in the micro-textures and in the composition of manganese-containing inclusions, found in all the analysed samples from Rome and Padua, suggest that the formation of this phase is not influenced by the chemical compositions of glassy matrix and opacifiers, reinforcing further the potential application of these inclusions as a technological marker of melting temperatures.

4.3. Colouring Elements

The glass tesserae from *S. Agnese fuori le mura* show the typical colourant elements, usually attested in other Roman and Medieval mosaics. In particular, cobalt (from 0.05 to 0.3 wt% as CoO) is identified in blue tesserae, copper (from 0.8 to 3.7 wt% as CuO) in turquoise, and green tesserae and manganese (from 1.3 to 2.3 wt% as MnO) in purple tesserae
(Table 2). In the opaque white/grey, yellow, and red/orange tesserae, the colours are due to the opacifiers, which act as pigments: Ca-antimonate and cassiterite for white/grey, Pb-antimonate for yellow, and metallic copper/cuprite for red/orange. In the case of *S. Agnese* tesserae, coloured by cobalt, this element is always coupled with copper (about 0.2 wt% as CuO), iron (Fe_2O_3 from 0.95 to 1.64 wt%), and lead (PbO from 0.15 to 0.7 wt%), in accordance with data reported for other blue tesserae from Roman mosaics dated from 5th to 12th cent. AD [25], suggesting similar source of colourant.

Gold tesserae of *S. Agnese* are all characterised by colourless and naturally coloured glass and, where present (SA Au8 and SA Au9), supporting tesserae and cartellina show the same colours and chemical composition. No opaque or strongly coloured gold glass is attested in *S. Agnese fuori le mura* (at least in the supposed original area of the mosaic). The gold tesserae characterised by supporting tesserae strongly coloured in yellow or green were identified in other coeval mosaics in Rome (i.e., *S. Sabina, S. Teodoro al Palatino,*

San Pietro in Vincoli, and *SS. Primo e Feliciano*), while gold tesserae with supporting tesserae made of opaque coloured glass (mainly red) are commonly attested in mosaics dated from 12th–13th cent. onwards in Rome and outside Rome [25].

In general, in all *S. Agnese* gold tesserae, colour is due to iron (Fe$_2$O$_3$: 0.6 ± 0.3 wt%), unintentionally introduced through the sand used. To produce a colourless glass, decolourant elements (antimony or manganese) must be added to the glass batch to mask the undesired colour of the naturally occurring iron. Antimony and manganese are the decolourants used in the Roman and Early Medieval periods. While the use of antimony as a decolourant goes from the first to the third century AD, the use of manganese continues even after the 4th century AD. In *S. Agnese* gold tesserae, the most common decolourant is manganese (SA Au4, SA Au5, SA Au6, SA Au7, SA Au8, and SA Au9), although antimony is identified in two gold tesserae (SA Au1 and SA Au3). The occurrence of antimony, manganese or both the elements in the gold tesserae from *S. Agnese* is particularly discriminant to identify the reference compositional groups and, therefore, to deduce their dating indirectly, as already discussed in Section 4.1.

In four gold tesserae (SA Au2, SA Au4, SA Au8, and SA Au9), gold foil is also present and SEM-EDS analyses showed that the gold foils of tesserae SA Au2, SA Au4, and SA Au8 are composed of pure gold (Au: 100 wt%), while that of tessera SA Au9 is composed of a gold/silver alloy (Au: 96.5 wt% and Ag: 3.5 wt%). A previous study carried out by Neri and Verità [73] demonstrated good matches between the compositions of the gold leaves and the analyses of contemporary gold coins in the Late Antique and Byzantine samples (3rd–9th cent. AD), suggesting that the leaves were made by beating circulating gold coins. This evidence may help a more precise dating of the tesserae. In the case of *S. Agnese* gold tesserae, the occurrence of foils composed of pure gold is not particularly significant because this composition of gold is diffused in coins from the Roman to early Medieval period. On the contrary, in the case of tessera SA Au9, the composition of the gold foil made of a gold/silver alloy, in particular, Au: 96.5 wt% and Ag: 3.5 wt%, revealed extremely important in the definition of the production date of this tessera. The composition of the gold foil of SA Au9 tesserae, in fact, matches perfectively with that of gold coins, circulating from 610 and 685, suggesting that tessera SA Au9 was produced appositely for the *S. Agnese* mosaic, commissioned by the Pope Honorius I, in charge from 625 to 638. A similar composition of gold foil was also found in gold tesserae from *SS. Primo e Feliciano* mosaic located in *S. Stefano Rotondo* church in Rome, coeval with that of *S. Agnese* [73] and this may indicate how for the realisation of the extended gold background of the early Medieval mosaics in Rome, gold tesserae were appositely produced. The analogy between the gold tesserae made for the apses of *S. Agnese* and *S. Stefano Rotondo* is also of particular interest, considering the differences in the execution technique and stylistic result of the two mosaics [3]. A fact that opens the way for further study of the entanglement between the supply and treatment of materials and the execution of mosaics in 7th-century Rome.

5. Conclusions

The opportunity of analysing glass tesserae from *S. Agnese fuori le mura* mosaic by means of an inter-disciplinary approach allowed us to add new data to the puzzle of Early Medieval Rome.

The various colours of tesserae were obtained using a skilful "mixing" among various glassy matrices, opacifiers/pigments, and colourants, typical of both the Roman and Late Antique/Early Medieval periods.

As regards the glassy matrices, they were all produced with natron as a flux in accordance with production technology of the 7th cent. AD, but in addition to compositions typical of the Roman period, Late Antique, and Early Medieval ones were also identified in *S. Agnese* tesserae. These showed a good match with the reference groups Foy 3.2, Foy 2.1, and HIMT, all supposed to have an Egyptian provenance. As in *S. Agnese* assemblage, the absence of tesserae having glassy matrices with Levantine provenance was already observed in the 5th–7th cent. glass mosaics from Ravenna/Classe [18]. This may suggest

that Rome and Ravenna supply glass tesserae for the realisation of LateAntique/Early Medieval mosaics by using similar trade routes. If coeval glass mosaics from other sites in the Mediterranean area are considered, the same trend is verified only for gold tesserae, while the new coloured and opaque tesserae were produced by using both Egyptian and Levantine glass [37].

As regards the opacifiers/pigments, Sb-based (Ca-antimonate and Pb-antimonate), Sn-based (cassiterite and Pb stannate), and Cu-based (metallic copper and cuprite) crystals were detected in various colours of *S. Agnese* tesserae. It should be stressed here how cassiterite was never attested until now as the main opacifier in Early Medieval mosaics from Rome but only in those of the Late Medieval age. Therefore, its findings in some *S. Agnese* tesserae demonstrated that the intentional use of cassiterite as an opacifier occurred in the 7th cent. AD, about 500 years in advance of the period previously established for the city of Rome. Grains of terracotta, identified in association with other opacifiers/pigments and not related to a specific colour, were also attested in *S. Agnese* tesserae, as well as in other mosaics of Rome, but this type of opacifier/pigment is few attested in other contexts, suggesting this as a possible local, as well as economic, technological choice to ample the colour palette. Based on the various habits of crystals and micro-textures and compositions of glassy matrices, both in situ and ex situ crystallisation methods of opacifiers were identified, and, in some cases, also thanks to the results of XRPD analyses, an estimation of melting temperatures is hypothesised. This experimental evidence allowed us to testify the multiple production technologies in the *S. Agnese* assemblage.

By combining the results obtained on glassy matrices and opacifiers/pigments of analysed tesserae, a quite complex "puzzle" was documented in *S. Agnese fuori le mura* mosaic because not only new-production tesserae, i.e., those probably produced ad hoc in the 7th century for the realisation of this mosaic, but also those obtained from re-using or recycling previous glass were identified (Appendix A), as here detailed:

- **New-production tesserae** i.e., tesserae characterised by both glassy matrices (compositional groups Foy 2.1, Foy 3.2 and HIMT) and Sn-containing opacifiers/pigments typical of Late antique and Early Medieval period (19 of 46 tesserae): all grey (SA Gr1 and SA Gr2) and red/orange (SA A1, SA R1, SA R2 and SA R3), and the majority of gold (SA Au2, SA Au5, SA Au6, SA Au7, SA Au8, SA Au9), green (SA VCh1, SA VCh2, SA VCh3 and SA VS1), and purple (SA P2, SA P6 and SA R4).

- **Re-used tesserae**, i.e., tesserae characterised by both glassy matrices and opacifiers, typical of the Roman period (17 of 46 tesserae): all white (SA Bi1, SA Bi2, SA Bi3) and yellow (SA G1 and SA G2), four blue (SA B2, SA B6, SA B7, SA B9), three gold (SA Au1, SA Au3, SA Au4), three green (SA VCh4, SA VS2, SA VS3), and two purple (SA P1 and SA P4).

- **Recycled tesserae,** i.e., tesserae characterised by glassy matrix, Late Antique/Early Medieval in age (compositional groups Foy 2, Foy 3.2 and HIMT), and Sb-containing opacifiers, typical of the Roman period (10 of 46 tesserae): all turquoise (SA Tu1 and SA Tu2), the majority of blue (SA B1, SA B3, SA B4, SA B5, SA B8), two purple (SA P3 and SA P5), and one green (SA VCh5).

In *S. Agnese*, a prevalence of new production tesserae was attested in those colours more typical of Early Medieval mosaics such as gold, grey, red/orange and purple/pink. Interesting also to note that all blue and white tesserae were only obtained by means of recycling and re-using previous tesserae, and no new productions were identified in *S. Agnese* for those colours.

The *S. Agnese* archaeometric puzzle seems unusual in other coeval glass mosaics from Rome, where a general preference to recycling and re-using previous glass tesserae is documented, but systematic comparisons and additional analyses by using similar methodological approach are still necessary to confirm this trend.

Therefore, further archaeometric studies on glass mosaics, within the inter-disciplinary research project on Medieval Rome funded by the Swiss National Science Foundation, are planned in the near future. Through the integration of new data and those so far published,

the ultimate goal of this inter-disciplinary research project is to broaden the understanding of the processes of production and circulation of glass tesserae in the early Middle Ages and, therefore, of the exchanges between Rome and the various areas of the Mediterranean in the period considered, emphasising the potentiality of the glass of uncovering the technical and socio-cultural knowledge that underpins their manufacturing, use, re-use, and recycling in the Early Medieval Rome.

Appendix A

Table A1. The main archaeometric results obtained on glass tesserae from *S. Agnese fuori le mura* mosaic.

Colour Macro-Group	Sample	Colour	Diaphaneity	Colouring Elements (+Decolourants)	Opacifier/Gold Foil	Reference Compositional Groups of Glassy Matrix	NOTES
Gold	SA Au1	Pale yellow-green	transparent	Iron (+Sb and very low Mn)	no gold foil	Roman	RE-USE
	SA Au2	Colourless	transparent	iron (+Mn and very low Sb)	gold foil: 100 wt% Au	Foy 3.2	NEW-PRODUCTION
	SA Au3	Colourless	transparent	Iron (+Sb and very low Mn)	no gold foil	Roman	RE-USE
	SA Au4	Colourless	transparent	Iron (+Mn)	gold foil: 100 wt% Au	Roman	RE-USE
	SA Au5	Colourless	transparent	Iron (+Mn)	no gold foil	Foy 3.2	NEW-PRODUCTION
	SA Au6	Colourless	transparent	Iron (+Mn)	no gold foil	Foy 3.2	NEW-PRODUCTION
	SA Au7	Pale green	transparent	Iron (+Mn)	no gold foil	Foy 3.2	NEW-PRODUCTION
	SA Au8	Pale green	transparent	Iron (+Mn)	golf foil: 100 wt% Au	Foy 3.2	NEW-PRODUCTION
	SA Au9	Colourless	transparent	Iron (+Mn)	gold foil: 96.5 wt% Au and 3.5 wt% Ag	HIMT	NEW-PRODUCTION
Blue	SA B1	blue	opaque	Cobalt	abundant Ca-antimonate (euhedral habit)	Foy 3.2	RECYCLING
	SA B2	blue	opaque	Cobalt	abundant Ca-antimonate (euhedral habit)	Roman	RE-USE
	SA B3	blue	semi-opaque	Cobalt	rare Ca-antimonate + bubbles	HIMT	RECYCLING
	SA B4	blue	semi-opaque	Cobalt	rare Ca-antimonate + bubbles	Foy 2.1	RECYCLING
	SA B5	blue	semi-opaque	Cobalt	rare Ca-antimonate + bubbles	Foy 3.2	RECYCLING
	SA B6	blue	opaque	Cobalt	abundant Ca-antimonate (euhedral habit)	Roman	RE-USE
	SA B7	blue	opaque	Cobalt	abundant Ca-antimonate (euhedral habit)	Roman	RE-USE
	SA B8	blue	semi-opaque	Cobalt	rare Ca-antimonate + bubbles	Foy 2.1	RECYCLING
	SA B9	blue	opaque	Cobalt	abundant Ca-antimonate (euhedral habit)	Roman	RE-USE
	SA Tu1	turquoise	opaque	Copper	abundant Ca-antimonate (rosary-shaped)	Foy 3.2	RECYCLING
	SA Tu2	turquoise	opaque	Copper	abundant Ca-antimonate (rosary-shaped)	Foy 3.2	RECYCLING

Table A1. *Cont.*

Colour Macro-Group	Sample	Colour	Diaphaneity	Colouring Elements (+Decolourants)	Opacifier/Gold Foil	Reference Compositional Groups of Glassy Matrix	NOTES
White	SA Bi1	white	opaque		abundant Ca-antimonate (euhedral habit)	High Mg glass	RE-USE
	SA Bi2	white	opaque		abundant Ca-antimonate (euhedral habit)	High Mg glass	RE-USE
	SA Bi3	white	opaque		abundant Ca-antimonate (euhedral habit)	High Mg glass	RE-USE
	SA Gr1	grey	opaque		abundant cassiterite	Foy 2.1	NEW-PRODUCTION
	SA Gr2	grey	opaque		abundant cassiterite	Foy 2.1	NEW-PRODUCTION
Purple	SA P1	purple	opaque	Manganese	abundant Ca-antimonate (euhedral habit)	Roman	RE-USE
	SA P2	dark purple	semi-opaque	Manganese	bubbles + sporadic cassiterite	HIMT	NEW-PRODUCTION
	SA P3	pale purple-pink	semi-opaque	Manganese	rare Ca-antimonate + bubbles + quartz + terracotta grains	Roman	RECYCLING
	SA P4	greyish purple	opaque	Manganese	abundant Ca-antimonate (euhedral habit)	Roman	RE-USE
	SA P5	pale purple-pink	semi-opaque	Manganese	rare Ca-antimonate + bubbles + quartz + terracotta grains	Foy 3.2	RECYCLING
	SA P6	dark purple	translucent	Manganese		HIMT	NEW-PRODUCTION
	SA R4	purple	translucent	Manganese		Foy 3.2	NEW-PRODUCTION
Green	SA VCh1	pale green	opaque	Copper	Pb-stannate	HIMT	NEW-PRODUCTION
	SA VCh2	pale green	opaque		Pb-stannate	HIMT	NEW-PRODUCTION
	SA VCh3	pale green	opaque	Copper	Pb-stannate	HIMT	NEW-PRODUCTION
	SA VCh4	pale green	opaque		Pb-antimonate	Roman	RE-USE
	SA VCH5	pale green	opaque	Copper	Pb-antimonate + terracotta grains + rare Ca-antimonate (rosary-shaped) + rare cassiterite	Foy 2.1	RECYCLING
	SA VS1	dark green	opaque	Copper	Pb-stannate	Foy 2.1	NEW-PRODUCTION
	SA VS2	dark green	opaque	Copper	Pb-antimonate	Roman	RE-USE
	SA VS3	dark green	opaque	Copper	Pb-antimonate	Roman	RE-USE
Yellow	SA G1	yellow	opaque		Pb-antimonate	Roman	RE-USE
	SA G2	yellow	opaque		Pb-antimonate	Roman	RE-USE
Red	SA A1	orange	opaque		cuprite	Foy 2.1	NEW-PRODUCTION
	SA R1	dark red	opaque		metallic copper	Foy 2.1	NEW-PRODUCTION
	SA R2	red	opaque		metallic copper	Foy 2.1	NEW-PRODUCTION
	SA R3	red	opaque		metallic copper	High Mg-P glass	NEW-PRODUCTION

References

1. Andaloro, M.; D'Angelo, C. (Eds.) *Mosaici Medievali a Roma Attraverso Il Restauro Dell'ICR (1991–2004)*; Gangemi Editore: Roma, Italy, 2017; ISBN 9788849232882.
2. Duchesne, L. *Le Liber Pontificalis*; Biblioth. des les franç. d'Athènes et de Rome; E. Thorin: Paris, France, 1886; p. 323.
3. Croci, C.; Gianandrea, M. L'abside Di Sant'Agnese Fuori Le Mura: Uno Sguardo Tra Passato e Futuro. In *Una Finestra su Roma Altomedievale: Pitture e Mosaici*; Croci, C., Gianandrea, M., Quadri, I., Romano, S., Eds.; Viella: Roma, Italy, 2022; pp. 129–153, ISBN 9788833138725.
4. Gianandrea, M. Il "Doppio Papa" Nelle Decorazioni Absidali Del Medioevo Romano. In *Le Plaisir de L'art du Moyen Âge: Commande, Production et Réception de L'œuvre D'art Mélanges en Hommage à Xavier Barral i Altet*; Alcoy, R., Allios, D., Eds.; A&J Picard: Paris, France, 2012; pp. 663–669, ISBN 978-2708409200.
5. Ballardini, A. Habeas Corpus: Agnese Nella Basilica Di via Nomentana. In *Di Bisanzio Dirai ciò che è Passato, che Passa e che Sarà; Scritti in Onore di Alessandra Guiglia*; Pedone, S., Paribeni, A., Eds.; Bardi Edizioni: Rome, Italy, 2018; pp. 253–279, ISBN 9788894810189.
6. Foletti, I.; Lešák, M.F. Hidden Treasure and Precious Pearl: Sant'Agnese Fuori Le Mura, Its Apse Mosaic, and the Experience of Liturgy. In *From Words to Space. Textual Sources for Reconstructing and Understanding Medieval Sacred Spaces*; De Blaauw, S., Scirocco, E., Eds.; Biblioteca Herziana: Rome, Italy, 2023; pp. 75–96, ISBN 979-12-80956-20-0.
7. Schüppel, K. «Claritate Fulgent et Puritate Translucent». Das Apsismosaik von Sant'Agnese Fuori Le Mura in Rom Aus Materialitätsperspektive. In *Visual and Material Cultures of Female Sanctity in Late Antiquity and the Middle Ages*; Schüppel, K., Ed.; Bamberg University Press: Bamberg, Germany, 2024.
8. Deiana, R.; Silvestri, A.; Gianandrea, M.; Maltoni, S.; Croci, C. The Medieval Glass Mosaic of S. Agnese Fuori Le Mura in Rome: Multispectral Imaging for Preliminary Identification of Original Tesserae. *Heritage* **2023**, *6*, 2851–2862. [CrossRef]
9. Silvestri, A.; Tonietto, S.; Molin, G.; Guerriero, P. Multi-Methodological Study of Palaeo-Christian Glass Mosaic Tesserae of St. Maria Mater Domini (Vicenza, Italy). *Eur. J. Mineral.* **2015**, *27*, 225–245. [CrossRef]
10. Cantone, V.; Deiana, R.; Silvestri, A.; Angelini, I. Obsidian and Obsidian-like Glass Tesserae: A Multidisciplinary Approach to Study the Dedication Wall Mosaic in the Church of St. Mary of the Admiral in Palermo (12th Century). *Open Archaeol.* **2020**, *6*, 403–416. [CrossRef]
11. Brill, R.H. *Chemical Analyses of Early Glasses. Volume 2 Tables of Analyses*; The Corning Museum of Glass: Corning, NY, USA, 1999; ISBN 0-872900-143-2.
12. Savitzky, A.; Golay, M.J.E. Smoothing and Differentiation of Data by Simplified Least Squares Procedures. *Anal. Chem.* **1964**, *36*, 1627–1639. [CrossRef]
13. Fiori, C.; Vandini, M.; Mazzotti, V. Colour and Technology of Mosaic "Glazes" in the Justinian and Theodora's Panels of the Basilica of San Vitale in Ravenna. *Ceramurgia* **2003**, *33*, 135–154.
14. Silvestri, A.; Tonietto, S.; Molin, G.; Guerriero, P. The Palaeo-Christian Glass Mosaic of St. Prosdocimus (Padova, Italy): Archaeometric Characterisation of Tesserae with Copper-or Tin-Based Opacifiers. *J. Archaeol. Sci.* **2014**, *42*, 51–67. [CrossRef]
15. Cariolaro, G.; Pierobon, G. *Teoria Della Probabilità e Dei Processi Aleatori—Vol. I—Probabilità e Variabili Aleatorie*; Collana di Elettrotecnica Generale ed Applicata; Patron Editore: Bologna, Italy, 1981; ISBN 9788855515559.
16. Maltoni, S.; Silvestri, A.; Molin, G. Opaque Red Glass Tesserae from Roman and Early-Byzantine Sites of North-Eastern Italy: New Light on Production Technologies. In Proceedings of the Annales du 20e Congrès de l'Association Internationale pour l'Histoire du Verre, Fribourg, Romont, Switzerland, 7–11 September 2015; Wolf, S., de Pury-Gysel, A., Eds.; Verlag Marie Leidorf GmbH: Rahden/Westfalen, Germany, 2017; pp. 280–287.
17. Paynter, S. Experiments in the Reconstruction of Roman Wood-Fired Glassworking Furnaces: Waste Products and Their Formation Processes. *J. Glass Stud.* **2008**, *50*, 271–290.
18. Fiorentino, S.; Chinni, T.; Vandini, M. Ravenna, Its Mosaics and the Contribution of Archaeometry. A Systematic Reassessment on Literature Data Related to Glass Tesserae and New Considerations. *J. Cult. Herit.* **2020**, *46*, 335–349. [CrossRef]
19. Schibille, N.; Freestone, I.C. Composition, Production and Procurement of Glass at San Vincenzo Al Volturno: An Early Medieval Monastic Complex in Southern Italy. *PLoS ONE* **2013**, *8*, e76479. [CrossRef]
20. Schibille, N.; Boschetti, C.; Valero Tévar, M.Á.; Veron, E.; de Juan Ares, J. The Color Palette of the Mosaics in the Roman Villa of Noheda (Spain). *Minerals* **2020**, *10*, 272. [CrossRef]
21. Tesser, E.; Verità, M.; Lazzarini, L.; Falcone, R.; Saguì, L.; Antonelli, F. Glass in Imitation of Exotic Marbles: An Analytical Investigation of 2nd Century AD Roman Sectilia from the Gorga Collection. *J. Cult. Herit.* **2020**, *42*, 202–212. [CrossRef]
22. Di Febo, R.; Casas, L.; Silvestri, A.; del Campo, Á.A.; Vallcorba, O.; Queralt, I.; Oró, J.; Villa, M.; Gàzquez, J.; Rius, J.; et al. Through the Looking Glass: Technological Characterization of Roman Glasses Mimicking Precious Stones from the Gorga Collection (Museo Nazionale Romano—Palazzo Altemps). *Minerals* **2023**, *13*, 1421. [CrossRef]
23. Henderson, J. Chemical Characterization of Roman Glass Vessels, Enamels and Tesserae. In Proceedings of the Materials Research Society Symposium, San Francisco, CA, USA, 17–21 April 1990; Materials Research Society: Pittsburgh, PA, USA, 2011; Volume 185, pp. 601–607.
24. Wypyski, M.T.; Becker, L. Glassmaking Tecnology at Antioch. In *The Arts of Antioch: Art Historical and Scientific Approaches to Roman Mosaics and a Catalogue of the Worcester Art Museum Antioch Collection*; Becker, L., Kondoleon, C., Eds.; Princeton University Press: Princeton, NJ, USA, 2005; pp. 115–175, ISBN 9780691122328.

25. Verità, M. Le Tessere Vitree Dei Mosaici Medievali a Roma. Tecnologia e Degrado. In *Mosaici Medievali a Roma Attraverso il Restauro dell'ICR (1991–2004)*; Andaloro, M., D'Angelo, C., Eds.; Gangemi Editore: Roma, Italy, 2017; pp. 437–477, ISBN 978-88492-3288-2.
26. Freestone, I.C. Glass Production in the First Millennium CE: A Compositional Perspective. In *Künstlichen Stein zum Durchsichtigen Massenprodukt/From Artificial Stone to Translucent Mass-Product. Berlin Studies of the Ancient World 67*; Klimscha, F., Karlsen, H.J., Hansen, S., Renn, J., Eds.; Edition Topoi: Berlin, Germany, 2021; pp. 245–263, ISBN 978-3-9819685-5-2.
27. Schibille, N. *Islamic Glass in the Making: Chronological and Geographical Dimensions*; Leuven University Press: Leuven, Belgium, 2022; Volume 7, ISBN 9789462703193.
28. Silvestri, A.; Gallo, F.; Maltoni, S.; Degryse, P.; Ganio, M.; Longinelli, A.; Molin, G. Things That Travelled—A Review of the Roman Glass from Northern Adriatic Italy. In *Things That Travelled: Mediterranean Glass in the First Millennium CE*; Rosenow, D., Phelps, M., Meek, A., Freestone, I.C., Eds.; UCL Press: London, UK, 2018; pp. 346–367, ISBN 978-1-78735-117-2.
29. Foy, D.; Picon, M.; Vichy, M.; Thirion-Merle, V. Caractérisation Des Verres de La Fin de l'Antiquité En Méditerranée Occidentale: L'émergence de Nouveaux Courants Commerciaux. In *Proceedings of the Echanges et Commerce du Verre dans le Monde Antique, Actes du Colloque de l'Association Francaise pour l'Archéologie du Verre, Aix-en-Provence et Marseille, France, 7–9 June 2001*; Foy, D., Nenna, M.-D., Eds.; Editions Monique Mergoil: Montagnac, France, 2003; pp. 41–85.
30. Foster, H.E.; Jackson, C.M. The Composition of 'Naturally Coloured' Late Roman Vessel Glass from Britain and the Implications for Models of Glass Production and Supply. *J. Archaeol. Sci.* **2009**, *36*, 189–204. [CrossRef]
31. Silvestri, A.; Tonietto, S.; Molin, G. The Palaeo-Christian Glass Mosaic of St. Prosdocimus (Padova, Italy): Archaeometric Characterisation of 'Gold' Tesserae. *J. Archaeol. Sci.* **2011**, *38*, 3402–3414. [CrossRef]
32. Maltoni, S.; Silvestri, A.; Marcante, A.; Molin, G. The Transition from Roman to Late Antique Glass: New Insights from the Domus of Tito Macro in Aquileia (Italy). *J. Archaeol. Sci.* **2016**, *73*, 1–16. [CrossRef]
33. Maltoni, S.; Gallo, F.; Silvestri, A.; Vandini, M.; Chinni, T.; Marcante, A.; Molin, G.; Cirelli, E. *Consumption, Working and Trade of Late Antique Glass from North Adriatic Italy: In Things That Travelled: Mediterranean Glass in the First Millennium CE*; Rosenow, D., Phelps, M., Meek, A., Freestone, I.C., Eds.; UCL Press: London, UK, 2018; pp. 191–214, ISBN 978-1-78735-117-2.
34. Balvanović, R.; Šmit, Ž. Sixth-Century AD Glassware from Jelica, Serbia—An Increasingly Complex Picture of Late Antiquity Glass Composition. *Archaeol. Anthropol. Sci.* **2020**, *12*, 94. [CrossRef]
35. Balvanović, R.V.; Šmit, Ž. Emerging Glass Industry Patterns in Late Antiquity Balkans and Beyond: New Analytical Findings on Foy 3.2 and Foy 2.1 Glass Types. *Materials* **2022**, *15*, 1086. [CrossRef]
36. Foster, H.E.; Jackson, C.M. The Composition of Late Romano-British Colourless Vessel Glass: Glass Production and Consumption. *J. Archaeol. Sci.* **2010**, *37*, 3068–3080. [CrossRef]
37. Gallo, F.; Marcante, A.; Silvestri, A.; Molin, G. The Glass of the "Casa Delle Bestie Ferite": A First Systematic Archaeometric Study on Late Roman Vessels from Aquileia. *J. Archaeol. Sci.* **2014**, *41*, 7–20. [CrossRef]
38. Maltoni, S.; Chinni, T.; Vandini, M.; Cirelli, E.; Silvestri, A.; Molin, G. Archaeological and Archaeometric Study of the Glass Finds from the Ancient Harbour of Classe (Ravenna-Italy): New Evidence. *Herit. Sci.* **2015**, *3*, 13. [CrossRef]
39. Schibille, N.; Sterrett-Krause, A.; Freestone, I.C. Glass Groups, Glass Supply and Recycling in Late Roman Carthage. *Archaeol. Anthropol. Sci.* **2017**, *9*, 1223–1241. [CrossRef]
40. Silvestri, A.; Maltoni, S.; Serra, C.L. Searching for Insights on Production Technologies in the Late-Antique/Byzantine Period: Glass Tesserae from Tyana (Cappadocia, Turkey). *J. Archaeol. Sci. Rep.* **2022**, *42*, 103381. [CrossRef]
41. Barfod, G.H.; Freestone, I.C.; Lesher, C.E.; Lichtenberger, A.; Raja, R. 'Alexandrian' Glass Confirmed by Hafnium Isotopes. *Sci. Rep.* **2020**, *10*, 11322. [CrossRef] [PubMed]
42. Tite, M.S.; Pradell, T.; Shortland, A.J. Discovery, Production and Use of Tin-Based Opacifiers in Glasses, Enamels and Glazes from the Late Iron Age Onwards: A Reassessment. *Archaeometry* **2008**, *50*, 67–84. [CrossRef]
43. Schibille, N.; Meek, A.; Tobias, B.; Entwistle, C.; Avisseau-Broustet, M.; Da Mota, H.; Gratuze, B. Comprehensive Chemical Characterisation of Byzantine Glass Weights. *PLoS ONE* **2016**, *11*, e0168289. [CrossRef]
44. Ceglia, A.; Cosyns, P.; Schibille, N.; Meulebroeck, W. Unravelling Provenance and Recycling of Late Antique Glass from Cyprus with Trace Elements. *Archaeol. Anthropol. Sci.* **2019**, *11*, 279–291. [CrossRef]
45. Silvestri, A.; Tonietto, S.; Molin, G.; Guerriero, P. The Palaeo-Christian Glass Mosaic of St. Prosdocimus (Padova, Italy): Archaeometric Characterisation of Tesserae with Antimony- or Phosphorus-Based Opacifiers. *J. Archaeol. Sci.* **2012**, *39*, 2177–2190. [CrossRef]
46. de Juan Ares, J.; Schibille, N.; Vidal Molina, J.; Sanchez de Prado, M.D. The Supply of Glass at *Portus Ilicitanus* (Alicante, Spain): A Meta-Analysis of HIMT Glasses. *Archaeometry* **2019**, *61*, 647–662. [CrossRef]
47. Freestone, I.C.; Hughes, M.J.; Stapleton, C.P. The Composition and Production of Anglo-Saxon Glass. In *Catalogue of Anglo-Saxon Glass in the British Museum*; Museum, B., Evison, V.I., Freestone, I.C., Eds.; The British Museum: London, UK, 2008; pp. 29–46. ISBN 9780861591671.
48. Mirti, P.; Lepora, A.; Saguì, L. Scientific Analysis of Seventh-Century Glass from the Crypta Balbi in Rome. *Archaeometry* **2000**, *42*, 359–374. [CrossRef]
49. Mirti, P.; Davit, P.; Gulmini, M.; Saguì, L. Glass Fragments from the Crypta Balbi in Rome: The Composition of Eighth-century Fragments. *Archaeometry* **2001**, *43*, 491–502. [CrossRef]
50. Cholakova, A.; Rehren, T.; Freestone, I.C. Compositional Identification of 6th c. AD Glass from the Lower Danube. *J. Archaeol. Sci. Rep.* **2016**, *7*, 625–632. [CrossRef]

51. Freestone, I.C. Chemical Analysis of "Raw" Glass Fragments. In *Excavation at Carthage, The Circular Harbour, North Side. the Site and Finds Other than Pottery*; Hurst, H.R., Ed.; British Academy Monographs in Archeology; Oxford University Press: Oxford, UK, 1994; Volume II, p. 290, ISBN 0-19-727003-4.

52. Nenna, M.-D. Egyptian Glass Abroad: HIMT Glass and Its Markets. In *Neighbours and Successors of Rome: Traditions of Glass Production and Use in Europe and the Middle East in the Later 1st Millennium AD*; Keller, D., Price, J., Jackson, C.M., Eds.; Oxbow Books: Oxford, UK, 2014; pp. 177–193, ISBN 9781782973973.

53. Freestone, I.C.; Degryse, P.; Lankton, J.; Gratuze, B.; Schneider, J. HIMT, Glass Composition and Commodity Branding in the Primary Glass Industry. In *Things that Travelled: Mediterranean Glass in the First Millennium AD*; Rosenow, D., Phelps, M., Meek, A., Freestone, I.C., Eds.; UCL Press: London, UK, 2018; pp. 159–190, ISBN 978-1-78735-117-2.

54. Drünert, F.; Palamara, E.; Zacharias, N.; Wondraczek, L.; Möncke, D. Ancient Roman Nano-Technology: Insight into the Manufacture of Mosaic Tesserae Opacified by Calcium Antimonate. *J. Eur. Ceram. Soc.* **2018**, *38*, 4799–4805. [CrossRef]

55. Lahlil, S.; Biron, I; Galoisy, L.; Morin, G. Rediscovering Ancient Glass Technologies through the Examination of Opacifier Crystals. *Appl. Phys. A* **2008**, *92*, 109–116. [CrossRef]

56. Lahlil, S.; Biron, I.; Cotte, M.; Susini, J.; Menguy, N. Synthesis of Calcium Antimonate Nano-Crystals by the 18th Dynasty Egyptian Glassmakers. *Appl. Phys. A* **2010**, *98*, 1–8. [CrossRef]

57. Lahlil, S.; Biron, I.; Cotte, M.; Susini, J. New Insight on the in Situ Crystallization of Calcium Antimonate Opacified Glass during the Roman Period. *Appl. Phys. A* **2010**, *100*, 683–692. [CrossRef]

58. Boschetti, C.; Leonelli, C.; Rosa, R.; Romagnoli, M.; Valero Tévar, M.Á.; Schibille, N. Preliminary Thermal Investigations of Calcium Antimonate Opacified White Glass Tesserae. *Heritage* **2020**, *3*, 549–560. [CrossRef]

59. Maltoni, S.; Silvestri, A. A Mosaic of Colors: Investigating Production Technologies of Roman Glass Tesserae from Northeastern Italy. *Minerals* **2018**, *8*, 255. [CrossRef]

60. Maltoni, S.; Silvestri, A. Innovation and Tradition in the Fourth Century Mosaic of the Casa Delle Bestie Ferite in Aquileia, Italy: Archaeometric Characterisation of the Glass Tesserae. *Archaeol. Anthropol. Sci.* **2016**, *10*, 415–429. [CrossRef]

61. Vandini, M.; Fiorentino, S. From Crystals to Color: A Compendium of Multi-Analytical Data on Mineralogical Phases in Opaque Colored Glass Mosaic Tesserae. *Minerals* **2020**, *10*, 609. [CrossRef]

62. Lahlil, S.; Cotte, M.; Biron, I.; Szlachetko, J.; Menguy, N.; Susini, J. Synthesizing Lead Antimonate in Ancient and Modern Opaque Glass. *J. Anal. At. Spectrom.* **2011**, *26*, 1040–1050. [CrossRef]

63. Shortland, A.J. The Use and Origin of Antimonate Colorants in Early Egyptian Glass. *Archaeometry* **2002**, *44*, 517–530. [CrossRef]

64. Mass, J.L.; Stone, R.E.; Wypyski, M.T. The Mineralogical and Metallurgical Origins of Roman Opaque Colored Glasses. In *Prehistory and History of Glassmaking Technology*; McCray, P., Kingery, D.W., Eds.; American Ceramic Society: Columbus, OH, USA, 1998; pp. 121–145, ISBN 9781574980417.

65. Matin, M. Tin-Based Opacifiers in Archaeological Glass and Ceramic Glazes: A Review and New Perspectives. *Archaeol. Anthropol. Sci.* **2019**, *11*, 1155–1167. [CrossRef]

66. Noirot, C.; Cormier, L.; Schibille, N.; Menguy, N.; Trcera, N.; Fonda, E. Comparative Investigation of Red and Orange Roman Tesserae: Role of Cu and Pb in Colour Formation. *Heritage* **2022**, *5*, 2628–2645. [CrossRef]

67. Bandiera, M.; Verità, M.; Lehuédé, P.; Vilarigues, M. The Technology of Copper-Based Red Glass Sectilia from the 2nd Century AD Lucius Verus Villa in Rome. *Minerals* **2020**, *10*, 875. [CrossRef]

68. Freestone, I.C. Composition and Microstructure of Early Opaque Red Glass. In *Early Vitreous Material. British Museum Occasional Paper, 56*; Bimson, M., Freestone, I.C., Eds.; British Museum: London, UK, 1987; pp. 173–191, ISBN 9780861590568.

69. Freestone, I.C.; Stapleton, C.P.; Rigby, V. The Production of Red Glass and Enamel in the Late Iron Age, Roman and Byzantine Periods. In *Throught a Glass Brightly: Studies in Byzantine and Medieval Art and Archaeology Presented to David Buckton*; Entwistle, C., Buckton, D., Eds.; Oxbow Books: Oxford, UK, 2003; pp. 142–154, ISBN 978-1785702518.

70. Zecchin, L. *Vetro e Vetrai Di Murano: Studi Sulla Storia Del Vetro (Vol. I)*; Arsenale Editrice: Venezia, Italy, 1987; ISBN 88-7743-022-2.

71. Croci, C. Ancora Su Agnese. Riflessioni Sul Volto 'Petrificato' Nel Mosaico Onoriano Della Basilica Nomentana (625–638). In *Visual and Material Cultures of Female Sanctity in Late Antiquity and the Middle Ages*; Schüppel, K., Ed.; Bamberg University Press: Bamberg, Germany, 2024.

72. Silvestri, A.; Nestola, F.; Peruzzo, L. Manganese-Containing Inclusions in Late-Antique Glass Mosaic Tesserae: A New Technological Marker? *Minerals* **2020**, *10*, 881. [CrossRef]

73. Neri, E.; Verità, M. Glass and Metal Analyses of Gold Leaf Tesserae from 1st to 9th Century Mosaics. A Contribution to Technological and Chronological Knowledge. *J. Archaeol. Sci.* **2013**, *40*, 4596–4606. [CrossRef]